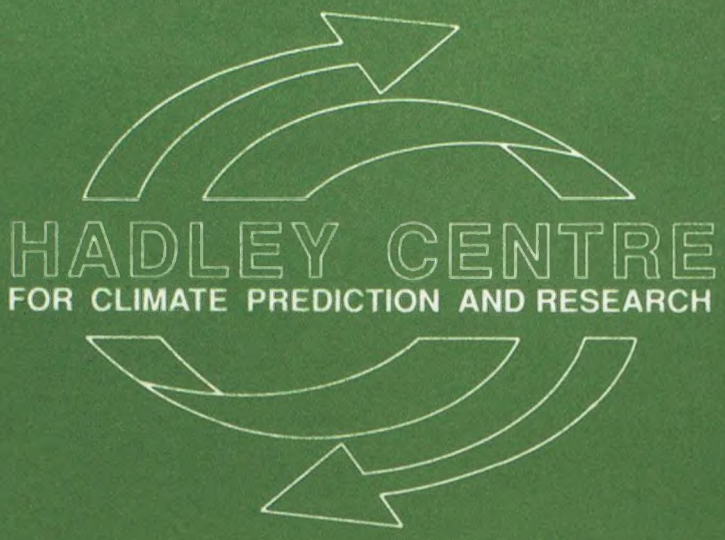

A consistent treatment of the evaporation of rain and snow for use in large-scale models

by

D Gregory

CRTN 55

March 1995

CLIMATE
RESEARCH
TECHNICAL
NOTE

Hadley Centre
Meteorological Office
London Road
Bracknell
Berkshire RG12 2SY

CLIMATE RESEARCH TECHNICAL NOTE NO. 55

A CONSISTENT TREATMENT OF THE EVAPORATION OF RAIN AND SNOW FOR USE IN LARGE-SCALE MODELS

by

D Gregory

Accepted for publication in the "Monthly Weather Review"

Hadley Centre for Climate Prediction and Research
Meteorological Office
London Road
Bracknell
Berkshire RG12 2SY

NOTE: This paper has not been published. Permission to quote from it should be obtained from the Director of the Hadley Centre.

ABSTRACT

The parametrisation of evaporation of rain and snow in large-scale numerical models of the atmosphere is considered. Precipitation rate dependent evaporation coefficients are derived following the method of Kessler for both stratiform and convective precipitation and compared with the calculations of more detailed models and observations using passive models. The derived 'bulk' parametrisations are in good agreement with the evaporation rates derived from the microphysical model of Clough and Franks (1991), showing more rapid evaporation of snow than rain. Comparison is made to other recent evaporation parametrizations and the sensitivity of the estimated evaporation rate to the nature of precipitation and the motion of the air through which it falls is also studied. The impact of the inclusion of different rates for the evaporation of stratiform rain and snow upon climate simulations by the Met. Office Unified Model (the Hadley Centre Climate Model) is considered.

1. INTRODUCTION

Much effort has been expended upon representing heat sources due to condensation within large-scale numerical models of the atmosphere. For large-scale stratiform cloud, the simple grid-box saturation schemes have been replaced in the latest generation of climate models with those which allow large-scale clouds to form before grid-box mean saturation with fractional cloud cover and cloud liquid water content being predicted prognostically (for example the scheme of Smith, 1990). Simplified microphysics are employed to calculate the fall out of precipitation. Similarly the initial use of convective adjustment schemes has been superceded by schemes employing simple cloud models developed from studies of field experiment data (for example GATE) and detailed numerical cloud models.

In comparison the sink of heat and source of moisture within the atmosphere due to the evaporation of rain and sublimation of snow has not received the same degree of attention. Although complex evaporation formula have been developed for use in numerical cloud models, many large-scale models still use a Kessler type formulation with a constant evaporation coefficient to calculate the rate of evaporation from the sub-saturation of the air through which the precipitation falls with no variation in the rate for rain and snow.

In recent years the representation of ice cloud processes has been highlighted as an area of uncertainty in general circulation models (for example see Senior and Mitchell, 1993) and the need to include improved parametrizations of cirrus clouds and their microphysics emphasised. Recent studies of meso-scale frontal dynamics have shown the importance of evaporatively driven circulation below regions of frontal ascent (Thorpe and Clough, 1991) and especially the evaporation of snow. Clough and Franks (1991) studied the difference in

evaporation rates of rain and snow in a microphysical model, showing that the rate of snow evaporation with time was twice as fast as that for rain of the same intensity.

Several authors have suggested improvements to evaporation parametrizations where the evaporation coefficient is dependent upon precipitation rate. Sundqvist (1988) obtained an evaporation coefficient for rain by integrating the rate equation for a single drop over the Marshall-Palmer distribution obtaining a coefficient dependent upon the square root of precipitation. Schlesinger et al (1988) developed a similar rate dependent coefficient using the radar observations of rainfall below convective clouds of Rosenfeld and Mintz(1988). Feingold (1993) is a further attempt, the parametrization being based upon the results from a one dimensional model of a downdraught with a detailed microphysics scheme included, the effect of the vertical velocity of the air through which the rain falls being included through a dependence on static stability. However all of these schemes treated rain and snow in the same manner. Only Heymsfield and Donner (1990) have suggested a parametrization for the evaporation of snow. They also point to the faster evaporation of snow than rain.

In this paper precipitation rate dependent evaporation coefficients are derived for both rain and snow (stratiform and convective) which are suitable for use in large-scale models of the atmosphere. The parametrisation builds upon the work of Clough and Franks (1991) who studied the difference between rain and snow evaporation using a detailed microphysical model. The performance of the scheme for the evaporation of stratiform precipitation is compared to their results and also against the parametrization schemes discussed above. In the case of convective precipitation, account is taken of the sub-grid scale nature of convection and the spatial variability of rainfall within such clouds. Results from Rosenfeld and Mintz (1988) are used to evaluate the performance of the scheme for convective

precipitation and the impact of the spatial variability of convective rain and vertical velocity upon the evaporation rate considered. Finally the impact of the larger evaporation rate of snow upon the simulation of climate by the UK Meteorological Office Unified Model is discussed.

2. THEORY OF EVAPORATION

The theory for the evaporation of a drop of water (or particle of ice) is well known (e.g. see Rogers and Yau, 1989);

$$\frac{dM(D)}{dt} = 2\pi D C_V D_a(T,p)(\rho_V - \rho_{VS}(T_W)) \qquad (1)$$

where M(D) is the mass of the drop of diameter D, C_v is a ventilation coefficient, $D_a(T)$ is the molecular diffusion coefficient at temperature T, ρ_v is the vapour density of water (subscript s indicating saturation value) and T_w is the wet bulb temperature (or ice bulb for snow) of the air through which the drop falls (at temperature T and mixing ratio q).

For non-spherical particles eqn(1) is valid, the diameter of the particle being replaced by the so called 'shape factor', C, generally smaller than D and so reducing the rate of evaporation. However in clouds ice crystals of different geometries often co-exist, a common form observed being an aggregation of different crystal types. Recent observations presented by Bower et al (1995) of ice crystal number concentrations in precipitating frontal cloud found that the number concentration of aggregates was 5 times higher than that of columns near the freezing level, other pristine crystals having much smaller number concentrations. Shapes of particles with sizes less than 150μm could not be determined by the technique used and these

were found to dominate the total ice crystal number concentration. However with such a complex mix of ice crystals within clouds it is difficult to include this effect of the "shape factor" in the parametrization and so equation (1) is used for both rain and snow.

In order to simplify the calculation and remove the dependence upon temperature and mixing ratio, Kessler(1969) approximated the relevant terms as;
to an accuracy of 25%. However he made no similar calculation for ice. In order to

$$D_a(T,p)(\rho_V-\rho_{VS}(T_w))=10^{-5}(\rho_V-\rho_{VS}(T)) \qquad (2)$$

represent accurately the evaporation processes a retention of the dependence of evaporation rate upon the temperature, pressure and mixing ratio of the drop environment seems desirable. However T_w cannot be calculated analytically, only by an iterative method. Such methods are not well suited to large-scale models of the atmosphere due to the time constraints imposed by the computational power available and so simpler approximations must be sought.

Consideration of the variation of

$$D_a(T,p)(\rho_V-\rho_{VS}(T_w))$$

with temperature, pressure and mixing ratio (appendix 1) leads to the approximate formula for the evaporation of a drop (or ice particle) ;

$$\frac{dM(D)}{dt}=2\pi DC_V A_V(T,p)(\rho_V-\rho_{VS}(T)) \qquad (3)$$

where $A_v(T,p)$ has a quadratic form with differing coefficients for water and ice. For water,

$$A_V^W(T,p)=(2.008\times10^{-9}T^2-1.385\times10^{-6}T+2.424\times10^{-4})\frac{10^5}{p} \quad (4a)$$

and for ice,

$$A_V^S(T,p)=(-5.2\times10^{-9}T^2+2.5332\times10^{-6}T-2.9111\times10^{-4})\frac{10^5}{p} \quad (4b)$$

where p is the pressure at the level of evaporation in pascals.

Equation (4b) has a root near 185K and so in practice the value of $A^S_V(T,p)$ below -50°C is fixed at the value appropriate at -50°C.

The errors introduced by the use of these approximate formulae are discussed in appendix 1, tending to increase towards saturation and freezing point but are considerably less than those introduced by Kessler's approximation.

The above formulae are applicable for a drop of given size. To obtain an expression for evaporation applicable for use in large-scale models equation (3) must be integrated over the entire spectrum of drop sizes, N(D),

$$\frac{dM}{dt}=2\pi A_V(T,p)(\rho_V-\rho_{VS}(T))\int_0^\infty DC_V(D)N(D)dD \quad (5)$$

where M is the total mass of precipitation.

This can be written in the form ,

$$\frac{dM}{dt}=\beta(\rho_V-\rho_{VS}(T)) \tag{6}$$

where β, the bulk evaporation coefficient is given by,

$$\beta=2\pi A_V(T,p)\int_0^\infty DC_V(D)N(D)dD \tag{7}$$

The population of droplets is usually approximated by a Marshall-Palmer drop size distribution (Marshall and Palmer 1948),

$$N(D)=N_0\exp(-\lambda D) \tag{8a}$$

where N_0 is the total number of particles per cubic metre and λ is the slope of the distribution. Some studies, for example that of Ulbrich (1983), have suggested that the distribution of drop sizes for rain is better approximated by a gamma distribution;

$$N(D)=N_0D^{\nu}\exp(-\lambda D) \tag{8b}$$

(see section 3(c) for further discussion).

The precipitation rate, P, is related to the mass of precipitation by,

$$P=VM \tag{9}$$

where V is the mass weighted fall speed over the droplet spectrum,

$$V=\frac{1}{M}\int_o^\infty v(D)M(D)N(D)dD \tag{10}$$

where v(D) is the fall speed of a particle of diameter D.

Equation (6) gives the rate of reduction in precipitation mass due to evaporation. However in large-scale models it is often more convenient to express evaporation in terms of a reduction in precipitation rate with height. It can be written that,

$$\frac{dP}{dz}=\frac{dP}{dt}\frac{dt}{dz}=\frac{1}{V}\frac{dP}{dt} \tag{11}$$

From eqn (9),

$$\frac{dP}{dt}=V\frac{dM}{dt}+M\frac{dV}{dt} \tag{12}$$

The form for V resulting from eqn (10) is usually AM^a (see section 3 below) and so eqn (12) can be simplified to,

$$\frac{dP}{dt}=(1+a)V\frac{dM}{dt} \tag{13}$$

and so from eqn (11),

$$\frac{dP}{dz}=(1+a)\frac{dM}{dt}=(1+a)\beta(\rho_v-\rho_{vs}(T)) \tag{14}$$

3. EVAPORATION OF STRATIFORM RAIN AND SNOW

Clough and Franks (1991) studied the evaporation of rain and snow using a microphysical model. They found that snow evaporates more rapidly than an equivalent mass of rain, the

principle factor controlling this behaviour being the lower bulk density of snow, leading to larger particles of a given mass and so greater evaporation rates (see equation (3)). In this section bulk evaporation coefficients are calculated for rain and snow using some of the assumed properties of precipitation used in Clough and Franks. The parametrization is compared against the results of their model and also with other parametrization schemes described in the introduction.

(a) Rain

The fall speed of rain used in these calculation is that suggested by Liu and Orville (1969) who performed a least squares fit on the analysis of Gunn and Kinzer's data (1949);

$$v(D)=842D^{0.8}\left(\frac{\rho_o}{\rho}\right)^{0.5} \qquad (15)$$

where ρ is the density of air and ρ_o a standard air density (taken to be $1kg/m^3$).

Frössling (1938) suggested a form for the ventilation coefficient of rain;

$$C_v=1+0.229Re^{0.5} \qquad (16)$$

where Re is the particle Reynolds number, given by $v(D)D\rho/\mu$, μ being the dynamic viscosity of air ($1.718\times10^{-5}kgm^{-1}s^{-1}$).

Substituting equation (16) into equation (7) gives after evaluation,

$$\beta=2\pi A_v^w(T,p)N_0\left(\frac{\Gamma(2)}{\lambda^2}+6.645\frac{(\rho\rho_0)^{0.25}}{\mu^{0.5}}\frac{\Gamma(2.9)}{\lambda^{2.9}}\right) \quad (17)$$

The slope of the distribution, λ, is related to the total mass of the precipitation;

$$M=\int_0^\infty M(D)dD=\int_0^\infty \rho_w\frac{4}{3}\pi\left(\frac{D}{2}\right)^3 N_0 e^{-\lambda D}dD=\frac{\Gamma(4)}{6}\rho_w\pi N_0\lambda^{-4} \quad (18)$$

where ρ_w is the density of water (1000kg/m^3).

Hence

$$\lambda=(\rho_w\pi N_0\Gamma(4)M^{-1}/6)^{0.25} \quad (19)$$

It is more usual in large-scale models for precipitation rate to be used rather than the mass of precipitation. These are related by equations (9) and (10) above. Substituting for v(D) from equation (15) into (10) gives the mass weighted fall speed as

$$V=\frac{842}{\lambda^{0.8}}\frac{\Gamma(4.8)}{\Gamma(4)}\left(\frac{\rho_0}{\rho}\right)^{0.5}=\frac{842}{(\rho_w\pi\Gamma(4)N_0/6)^{0.2}}\frac{\Gamma(4.8)}{\Gamma(4)}\left(\frac{\rho_0}{\rho}\right)^{0.5}M^{0.2}$$

$$=AM^{0.2} \quad (20)$$

Substituting for V into equation (9) gives after rearrangement,

$$M=(A^{-1})^{1/1.2}R^{1/1.2} \quad (21)$$

where R is the rainfall rate (kg/m^2/s).

Substitution into equation (17) using equation (19) and a value for N_0 of 6×10^6 m^{-4} (Ulbrich, 1983) gives β as,

$$\beta = A_v^w(T,p)(75.67(R\rho^{0.5})^{0.42} + 605.17\rho^{0.55}R^{0.60}) \quad (22)$$

(b) Snow

A similar analysis to that above can be carried out to yield a bulk evaporation coefficient for snow. Here the fall speed of snow is taken to be that suggested by Cox (1988) which was chosen to match the bulk-rainfall rate behaviour reported by Heymsfield (1977) over a wide range of ice-water contents;

$$v(D) = 16.2D^{0.527}\left(\frac{\rho_0}{\rho}\right)^{0.5} \quad (23)$$

Snow particles are non-spherical in shape and their density varies with size. Cox (1988) used the relationship,

$$M(D) = 0.078D^{2.1} \quad (24)$$

relating the mass of a particle to its mean diameter (after Locatelli and Hobbs (1974) - representative of assemblages of dendrites). These relationships for fall speed and particle mass correspond to case (e) of Clough and Franks (1991). The sensitivity of snow evaporation rates to assumptions regarding fall speeds and the density of particles is discussed in detail by Clough and Franks (1991) and briefly described in section 3(d).

The ventilation coefficient for snow was studied by Thorpe and Mason (1966) who derived

the expression,

$$C_V=0.65+0.44S_C^{1/3}Re^{0.5} \tag{25}$$

where S_c is the Schmidt number (0.6). This form is only strictly valid for hexagonal plates but was used by Cloud and Franks (1991) for all snow types in their study in the absence of laboratory observations for a diverse range of ice types. Although ventilation coefficients are known to vary with particle shape ice crystals (Pruppacher and Klett, 1978, figure 13-25), ice in clouds is often found to be a complex mix of different type crystals and it is therefore difficult to specify a general ventilation coefficient.

Substituting into equation (7) from equation (25) and evaluating,

$$\beta=2\pi A_V^S(T,p)N_0\left(\frac{0.65\Gamma(2)}{\lambda^2}+1.49\frac{(\rho\rho_0)^{0.25}}{\mu^{0.5}}\frac{\Gamma(2.7635)}{\lambda^{2.7635}}\right) \tag{26}$$

By a similar method to that used previously λ is given by,

$$\lambda=(0.078N_0\Gamma(3.1)M^{-1})^{1/3.1} \tag{27}$$

Evaluating the mass weighted fall speed from equations (10), (23) and (24) gives,

$$V=\frac{16.2}{\lambda^{0.527}}\frac{\Gamma(3.627)}{\Gamma(3.1)}\left(\frac{\rho_0}{\rho}\right)^{0.5}=\frac{16.2}{(0.078\Gamma(3.1)N_0)^{0.17}}\frac{\Gamma(3.627)}{\Gamma(3.1)}\left(\frac{\rho_0}{\rho}\right)^{0.5}M^{0.17}$$

$$=A'M^{0.17} \tag{28}$$

and so from equation (9)

$$M=(A'^{-1})^{1/1.17}S^{1/1.17} \tag{29}$$

where S is the snow fall rate ($kg/m^2/s$).

Substitution into equation (26) using equation (27) with a value of N_0 of $2x10^6$ m^{-4}(from Cox 1988) gives β as ,

$$\beta = A_V^S(T,p)(1765.55(S\rho^{0.5})^{0.55} + 34784.06\rho^{0.63}S^{0.76}) \quad (30)$$

(c) Comparison against Clough and Franks (1991)

Clough and Franks (1991) used a complex microphysical model to study the evaporation of rain and snow, finding that snow evaporated approximately twice as fast as rain. Figures 1(a) and 1(b) compare the rate of change of precipitation mass with time from their study and from the parametrizations of evaporation derived above using their initial conditions; an initial precipitation rate of 1mm/hr, a pressure of 850mb, a constant temperature of 0°C and constant relative humidity of 60%. The curve for snow is that calculated using the same fall speed and mass-diameter relationship used above (their case (e)).

For both rain and snow evaporation is over predicted by the scheme developed above. For rain this may be due to the assumed Marshall-Palmer distribution of drop sizes. Although Clough and Franks assumed this initially they found substantial deviations from it as time progresses caused by the rapid evaporation of small droplets, increasing the fractional mass of precipitation contained in the slower evaporating larger drops. Assuming a constant Marshall-Palmer distribution implies generation of small drops at a rate faster than they would be generated through the evaporation of larger drops.

Some correction for this can be included by the use of a gamma distribution to describe the drop size distribution (see equation (8b)). Several observational studies have suggested that this is a better fit for rainfall drop size spectra than the exponential fit assumed above (for example, Ulbrich, 1983; Willis, 1984). Ulbrich (1983) empirically determined that,

$$N_0=N_G\exp(3.2\nu) \tag{31}$$

where $N_G=6\text{x}10^4\text{x}10^{2(1+\nu)}\text{m}^{-3}\text{m}^{-1-\nu}$.

Ulbrich found ν to vary between -3 and 5 depending upon precipitation type. For stratiform rain the range was -1 to 4.5, while for thunderstorms ν had a range of between 0.4 and 1.5. Willis suggests a value of 2.5 based upon observations in a tropical cyclone. Setting ν equal to unity in equation (8b) and using this (together with equation (31)) rather than the Marshall-Palmer distribution in the above derivation results in a modified expression for the evaporation coefficient for rain;

$$\beta=2\pi A_V^{\,W}(T,p)N_0\left(\frac{\Gamma(3)}{\lambda^3}+6.645\frac{(\rho\rho_0)^{0.25}}{\mu^{0.5}}\frac{\Gamma(3.9)}{\lambda^{3.9}}\right) \tag{32a}$$

which on evaluation of constants and writing in terms of rainfall rate as previously becomes,

$$\beta=A_V^{\,W}(T,p)(122.68(R\rho^{0.5})^{0.52}+919.25\rho^{0.59}R^{0.67}) \tag{32a}$$

This gives a better fit against the results of Clough and Franks (figure 1). Table 1 compares the time required for 90% of the initial precipitation mass to evaporate from Clough and Franks study with that using the parametrized evaporation rate. Assuming a Marshall-Palmer distribution for the drop size spectrum results in a 25% underestimate of the fall distance by which 90% of the precipitation has evaporated. With a gamma distribution of order unity excellent agreement is found between the explicit evaporation model and parametrization.

Increasing the order of the gamma distribution to 2 and 4 leads to increased depths for evaporation of 90% of the initial rain mass of 890 and 1060m respectively, both in worse agreement with the explicit model calculations.

Considering the evaporation of snow, the parametrization over estimates the rate at which evaporation occurs. The fall distance for 90% of the initial mass of snow to be evaporated in under predicted by 25%, a similar amount to that of the parametrization for rain evaporation assuming a Marshall-Palmer drop size distribution. Clough and Frank (1991) report that as snow evaporates the particle size distribution follows the shape of the Marshall-Palmer distribution. Hence deviations from this cannot explain the overestimation in the evaporation rates as for rain. Indeed repeating the calculations using a gamma distribution to describe the snow size spectra brings no improvement in the comparison of parametrization and explicit model. However this disagreement is not as large as appears. After a fall distance by which the parametrization predicts that 90% of the initial snow mass is evaporated (240m), the model of Clough and Frank predicts that 80% of the initial mass is evaporated. Hence only a 10% error in the net amount of snow evaporated is introduced by the use of the bulk parametrization.

One possible explanation for the difference in the parametrized and explicitly modelled evaporation rates is the constant value of N_0 used in the derivation of the coefficients of equation (30). Several authors suggest that N_0 for snow varies as a function of precipitation mass and temperature. However results are contradictory. Based upon observations of falling snow near the ground, Sekhon and Srivastava (1970) report that N_0 is approximately inversely proportional to precipitation rate. However Houze et al (1979) in an analysis of particle size data collected in frontal clouds show that N_0 increases with precipitation mass. The later

study also found an increase of N_0 as temperature decreased. The contradictory nature of these observations may be due to their different natures, one being in cloud (Houze et al, 1979), the earlier observation (Sekhon and Srivastava, 1970) being of snow near the ground.

A decrease in N_0 as the mass of snow evaporates would tend to decrease the rate of evaporation and bring the parametrization into better agreement with Clough and Franks model. It would be possible to study how N_0 varies with precipitation rate using a model such as that employed in Clough and Frank (1991), but they provide no details. Because of the uncertainties discussed above, here N_0 for snow is kept constant although the sensitivity of the parametrization scheme to the temperature dependency of N_0 is investigated in section 3(d). It is recognised that this is a deficiency in the parametrization which is in need of further study using both observations and detailed microphysical models, although as discussed above it would appear to only cause errors of around 10% in the estimation of the amount of precipitation mass evaporated.

(d) Comparison with other parametrizations of evaporation

As discussed in the introduction several authors have suggested forms for the evaporation of rain for use in large-scale models, although only Heymsfield and Donner (1990) have suggested a difference between the evaporation of rain and snow. As the results in the previous section have shown this may result in an under-estimation of the sublimation of snow by a factor of two.

Sundqvist (1988) suggested the rate of evaporation of falling rain,

In deriving this parametrization Sundqvist assumes a constant fall speed of 5m/s and so this

$$\frac{dP}{dt}=10^{-5}q_s(T)(1-RH)P^{0.5} \tag{33}$$

can be converted into an expression for the change of precipitation with height due to evaporation,

$$\frac{dP}{dz}=0.2\times10^{-5}q_s(T)(1-RH)P^{0.5} \tag{34}$$

Schlesinger et al (1988) suggest

$$\frac{dP}{dz}=\frac{CP^{a}\Phi(z)}{(K_1+K_2)} \tag{35}$$

where $K_1= (L^2\rho_w)/(KR_vT^2)$

$K_2= (R_vT\rho_w)/(D_ae_s(T))$

and $\phi(z) =$ (1-RH) for stratiform clouds (assuming constant relative humidity below cloud base)

or $= \gamma/(\gamma+z)$ for convective cloud (assuming constant absolute humidity below cloud base)

with γ being the temperature lapse rate.

Constants C and a were derived by minimising the error between the parametrised evaporation rate and radar observations of rainfall below cloud base (Rosenfeld and Mintz (1988) in a study of convective clouds over South Africa). Values estimated by this procedure were 2.63×10^{-2} $[(mm/h)^{1-a}/(mm^3/s)]$ for C and 0.606 for a.

Figure 2 shows the reduction of rainfall rate as a function of z below cloud base for the same conditions used in the comparison in section 3(c) above. The parametrization

derived above delivers a similar result to that of Schlesinger et al (1988). As the latter was derived from observational data with different environmental conditions and precipitation rates than the model of Clough and Franks (1991) this indicates that the current parametrization is valid over a wide range of conditions. The scheme of Sundqvist (1988) underestimates the rate of evaporation of rain by 300% using the coefficient above suggesting that an increase in the value of the coefficient is necessary.

Heymsfield and Donner (1990) present a parametrization of evaporation of ice and water (at 0°C only) and note, as Clough and Franks (1991), the much shorter fall distance required for ice to sublimate completely. They estimate the fraction of the initial water content (FR) remaining after a distance z as,

$$FR=(1-\frac{z}{z_{max}})^2 \qquad (36)$$

where z_{max} is the maximum fall distance required to evaporate the largest size particle which contributes significantly to the initial water content. This is given by a complex function of ice water content with constants depending upon the phase of the condensate, relative humidity and temperature. Values of z_{max} were derived from a simple microphysical model similar to that used by Clough and Frank (1991). The form of eqn (33) was calculated from particle size spectra measurements representative of differing temperature and stability regimes. The assumed environment through which the water is assumed to fall is typical of that found in regions of ice sublimation below stratiform clouds, with the first 300m below cloud base being isothermal and relative humidity decreasing to a value RH; below this temperature increases at 9K/km with the relative humidity fixed at RH.

Figure 3 shows the depth at which the initial water content falling from cloud base is reduced

to 50% of the initial value for temperatures = 0, -20 and -40°C for various initial precipitation masses from the Heymsfield and Donner scheme and the parametrization for snow evaporation developed above (calculated assuming the precipitation falls through the same environment as specified by Heymsfield and Donner). Heymsfield and Donner's calculations were carried out at the pressure level of the observations (Heymsfield, personal communication). In the current calculations pressures typical of those at which these temperatures are observed are used, being 850, 550 and 350mb respectively. These were estimated from the US Standard Atmosphere (US Government Printing Office, 1976). Calculations were carried out for values of relative humidities (300m below the cloud base) between 20 and 80%. In their calculations there is no dependency of fall speed upon the density of the air and so this has been removed from the current parametrization (by removing the density terms of eqn (30)) for these comparisons.

For most of the conditions studied the current parametrization predicts larger fall distances for a 50% reduction in precipitation mass. Better agreement is seen at 0°C for low precipitation mass ($10^{-2}gm^{-2}$) but differences increase for relative humidities below 60% as mass increases. For an 80% relative humidity agreement is good for the two largest precipitation masses considered. At -20°C increasing differences between the two scheme are seen, with the current scheme showing fall distances for a 50% reduction in precipitation mass twice as large as Heymsfield and Donner's scheme for humidities of 60% and below, although good agreement between the two schemes is found for a relative humidity of 80%. At -40°C similar differences are found, again the current parametrization giving generally larger fall distances than those of the Heymsfield and Donner's scheme.

The difference in results may be caused by several of the assumptions used; fall speed, the

mass-diameter relationship for various types of snow used to estimate z_{max}, the initial particle size distribution chosen or the value, neglect of the "shape factor" for non-spherical particl es and variation of N_0 with temperature and precipitation mass. Heymsfield and Donner (1990) give few details of their calculation but appear to use different characteristics depending upon the temperature of the environment through which the snow falls and the nature of the precipitation observed. Clough and Franks (1991) calculate snow evaporation for several different types of snow, but these have sublimation rates which are slower than the type of snow assumed for the present calculations and, increase the fall distance for 95% evaporation of the initial snow mass by 30% over the snow type assumed in the parametrization (see table 1(b), Clough and Franks (1991)). Hence differences in fall speed and mass-diameter relationship appear to be unable to explain the differences of figure 3. Inclusion of a "shape factor" into equation (1) to account for non-spherical nature of snow particles would tend to reduce sublimation rates and increase fall distances for a 50% reduction of the initial snow mass.

In their calculations Heymsfield and Donner used particle size distributions based upon observations (but give no details) whereas here a constant Marshall-Palmer distribution has been used throughout. Clough and Franks (1991) report that large snow particles evaporate more rapidly, with the mean radius of the distribution decreasing with time for the type of snow assumed here. Assuming a constant Marshall-Palmer distribution of particle sizes the fraction of larger particles over a period of time must be overestimated, leading to an over estimation of the evaporation rate (see figure 1(b)). The faster evaporation rates of Heymsfield and Donner may imply an even larger proportion of large particles within their initial particle size distribution than the Marshall-Palmer distribution.

In a parametrization of ice phase microphysics Cox (1988), following the work of Houze et al (1979), includes a temperature dependence upon the number of particle per unit volume (N_0);

$$N_0=N_0(0)F(T)=N_0(0)\exp(\frac{(273.15-T)}{8.18}) \qquad (37)$$

where $N_0(0)$ is taken to be 2×10^{-6} m^{-3} (as in section 3(b) above). Houze et al (1979) comment that the lower values of N_0 towards the freezing level are due to the growth of ice particles as they fall through cloud. The temperature used in the above expression for the purposes of applying it to a parametrization of the sublimation of snow must be that of cloud base from which the snow falls into unsaturated air.

Including such a dependency results in a modified expression for the evaporation coefficient for snow;

$$\beta=A_V^S(T,p)(1765.55(S\rho^{0.5})^{0.55}F(T_b)^{0.45}+34784.06\rho^{0.63}S^{0.76}F(T_b)^{0.24}) \qquad (38)$$

where F(T) is the exponential function of equation (34) and T_b is the cloud base temperature.

Figure 4 compares the parametrization of Heymsfield and Donner (1990) with the revised treatment for the sublimation of snow (again ignoring any density dependence) for -20 and -40°C. Better agreement is seen for -20°C for relative humidities of 60% and below. At -40°C depths for a 50% reduction of precipitation mass are underestimated at 60% relative humidity and also precipitation masses greater than 10^{-1} gm^{-3}. Below 40% relative humidity and $10^{-1}gm^3$ agreement between the two schemes is reasonable.

As discussed previously Houze et al (1979) also report that the variation of N_0 with temperature is dependent upon the mass of the precipitation being measured, with larger increases with falling temperature being seen for a larger mass of precipitation. This would further reduce the evaporation depths shown in figure 4 for the scheme developed here and so not improve agreement between the two schemes. Ryan (1995) in a review of observations of precipitating layer cloud compares several estimates of the variation of N_0 with temperature. Little agreement is found, although most show an increase in N_0 with falling temperature. In view of this uncertainty these calculations should only be viewed as sensitivity studies. However it is clear from these results that the sublimation of snow is sensitive to the value of N_0. As suggested previously further observational and modelling studies are required in order to determine how this quantity varies with a range of parameters.

Heymsfield and Donner also present a parametrization of the evaporation of rain (at 0°C) using eqn (36). Figure 5 compares this with the parametrization developed in section 3(a) above. Fall distances for 50% evaporation of precipitation mass are smaller than for the parametrization developed earlier, as in general were the values for snow sublimation depths in figure 3. This suggests that the Heymsfield and Donner parametrization scheme may be over-estimating the rate of both evaporation and sublimation. Further analysis of observations and experimentation with detailed microphysical models is required if these differences are to be clarified.

4. EVAPORATION OF CONVECTIVE PRECIPITATION

(a) Sub-grid scale variability of rainfall

The form of the parametrization for the evaporation of rain and snow so far derived assumes that the rainfall rate is constant. While this may be a reasonable approximation for precipitation from stratiform cloud on the scale of a grid square of a large-scale model, convective precipitation exhibits a high degree of spatial variability. Although there are few observations which characterise this variability attempts have been made in the past to include this effect in the parametrisation of the interaction of precipitation and land surface processes (Warrilow et al (1986), Dolman and Gregory (1992)) by assuming that local precipitation rates are exponentially distributed within a rain area. This technique may also be applied to the treatment of evaporation of falling precipitation from convective clouds.

Assume that precipitation falls over an area A and that the fractional area covered by precipitation rates between P and P+dP is,

$$(P_0)^{-1}\exp(-\frac{P}{P_0})dP \qquad (39)$$

where P_0 is the mean precipitation rates within the wetted area and P is the local precipitation rate.

Integrating equation (6) over this distribution gives the mean rate of evaporation of precipitation mass,

$$\frac{dM}{dt}=\overline{\beta}(\rho_v-\rho_{vs}(T)) \tag{40}$$

with β, the mean bulk evaporation coefficient, given by

$$\overline{\beta}=\int_0^\infty \beta(P)(P_0)^{-1}e^{-\frac{P}{P_0}}dP \tag{41}$$

(β(P) being given by eqn (7)).

Evaluating eqn (41) using the same characteristics for rain as in section 3(c) (with a gamma distribution of order unity to describe the drop size distribution) and snow as in section 3(b) gives for rain,

$$\overline{\beta}=A_v^W(T,p)(108.80(R\rho^{0.5})^{0.52}+830.73\rho^{0.59}R^{0.67}) \tag{42a}$$

and for snow,

$$\overline{\beta}=A_v^S(T,p)(1569.52(S\rho^{0.5})^{0.55}+32069.02\rho^{0.63}S^{0.76}) \tag{42b}$$

Rosenfeld and Mintz (1988) present radar derived estimates for evaporation of rain below convective clouds for six values of rainfall at cloud base (Pb=0.26, 0.58, 1.2, 2.9, 6.2, 13.8mm/hr) derived from observations of around 2500 clouds. The cloud base was typically between 1 and 2.2km (above a plateau of 1700m height), with a mean cloud base temperature of 9°C. Schlesinger et al (1988) used these data to derive the parametrization of rainfall evaporation discussed in section 3(d) above.

Figure 6 compares the observations of Rosenfeld and Mintz (1988) with the parametrization of evaporation for rain derived in section 3(a), using the parametrization of eqns (22) and

(39a). Cloud base is assumed to be at 900mb, with a temperature of 9°C. Below cloud base a dry adiabatic lapse rate is assumed with specific humidity being kept constant from the value at cloud base (implying decreasing relative humidity towards the surface). As previously the model used in the calculation is passive, i.e. the impact of evaporation upon the air through which the rain falls is not included in the calculation.

For fall distances of 1km or less the parametrization produces rainfall rates which are within the errors of the observations (caused by both the spread of the rainfall data and errors in the radar derived rainfall rates), a closer fit being found for more intense rainfall rates. The impact of including the variability of convective precipitation over the rain area is small at all rainfall intensities.

(b) Impact of vertical velocity

In convective clouds the vertical velocity of the air through which precipitation falls may be similar to the fall speed of the drops and so equation (9) relating precipitation rate to the mass of precipitation must be modified;

$$P=(V+w)M \tag{43}$$

where w is the ambient vertical velocity. If w > -V then the precipitation rate is zero.

In section 3 the mass weighted fall velocity had the form AM^a and so equation (43) may be written as,

$$AM^{1+a}+Mw-P=0 \tag{44}$$

Given w and P this can be solved iteratively such that,

$$M=\alpha P \tag{45}$$

For the evaporation of rain using equations (32a) and the equivalent of equation (19) for a gamma distribution of order unity,

$$\lambda=(\frac{1}{6}\rho_w N_0 \pi \Gamma(5))^{0.2} M^{-0.2}$$

the evaporation coefficient β can be written as,

$$\beta=2\pi A_V^W(T,p)N_0(\frac{\Gamma(3)\alpha^{0.6}P^{0.6}}{(\rho_W N_0 \pi \Gamma(5)/6)^{0.6}}+6.645\frac{(\rho\rho_0)^{0.25}}{\mu^{0.25}}\frac{\Gamma(3.9)\alpha^{0.78}P^{0.78}}{(\rho_W N_0 \pi \Gamma(5)/6)^{0.78}}) \tag{46}$$

with N_0 given by equation (31) with ν set to unity.

As α is obtained by iteration this complicates the integration of equation (46) over a range of precipitation rates as in section 4(a) above. An alternative method is to integrate over a distribution of precipitation mass. Similarly to the method above it is assumed that the mass of precipitation is distributed over the rain area according to,

$$\frac{1}{M_0}\exp(-\frac{M}{M_0})dM \tag{47}$$

where M_0 is the area mean mass of precipitation and M is the local mass of precipitation.

Following equations (41) and (42) above,

$$\overline{\beta}=\int_0^{\infty}\beta(M)\frac{1}{M_0}e^{-\frac{M}{M_0}}dM \tag{48}$$

which following the analysis of section 3(c) above, with the drop size distribution described by a gamma function of order unity, gives,

$$\overline{\beta}=A_V^W(T,p)(454.93M_0^{0.6}+5415.66M_0^{0.78}) \tag{49}$$

M_0 is calculated from P_0 using equation (45) with the mean fall speed from equation (20) and the vertical velocity. For rain falling through stationary air, equation (49) yields identical evaporation rates as equation (32b). As downward vertical motion increases, the quantity of rain mass needed to give a constant precipitation rate is reduced. For a smaller mass of rain the Marshall-Palmer distribution implies a greater proportion of small droplets, which considering equation (3), are slower evaporating. Hence for a constant precipitation rate, as downward velocity increases, the evaporation rate decreases.

Figure 7 repeats the comparison against the observation of Rosenfeld and Mintz (1988) with downward moving vertical velocities of 0, 5, and 10 ms^{-1}. As expected evaporation rates are reduced at all rainfall intensities, with the impact increasing as the rainfall intensity is reduced. Care must be exercised as to whether the better fit to the observations for rainfall below 1mm/hr with downward motion is realistic as it must be questionable whether such strong downward motion would exist in these weak systems.

These results illustrate that inclusion of the influence of vertical velocity is important in determining accurate evaporation rates especially for the treatment of convective precipitation. However many convection schemes do not estimate such a variable (adjustment and Kuo

schemes). Schemes which use a simple cloud model to represent the effects of the updraught and downdraught do not necessarily need to predict the vertical velocity inside cloud (for example the scheme reported by Gregory and Rowntree (1990)). Also the simple entrainment hypothesis used by many one dimensional cloud models does not lead to an accurate determination of vertical velocity within convective cloud (see for example Curić and Janc, 1988).

Recognising these difficulties, Feingold (1993) attempts to overcome them by including a dependence of evaporation upon the stability of the atmosphere through which rain falls, which Srivastava (1985) (among others) have found to be important in determining the intensity of downdraught circulations (the downward velocity increasing as the lapse rate approached the dry adiabatic value). He used a multi-variate analysis to match results from a one dimensional model of a downdraught, incorporating a complex evaporation scheme, to evaluate coefficients in a parametrization of evaporation taking the form,

$$FE = a_0 X_{l0}^{a1} N_0^{a2} z^{a3} \gamma^{a4} \qquad (50)$$

where X_{lo}^{a1} is the precipitation mixing ratio at cloud base ($kgkg^{-1}$),

N_o is the drop number density (cm^{-3})

z is the distance fallen (m)

γ is the lapse rate (Kkm^{-1})

and FE is the fraction of precipitation evaporated after a distance z (%)

For a cloud base temperature of 10 deg C the coefficients of this expression were found to be; a0 = 0.0127,a1 = -0.0725, a2 = 0.214, a3 = 0.555, a4 = 2.217.

Using this parametrization little variation in evaporation rate is seen across the rainfall rates documented by Rosenfeld and Mintz (1988) (figure 8) - only 3% change in the amount of rain evaporated after 1000m over a 50 times increase in the rainfall rate. This is due to the small value for a1 in Feingold's parametrization. For a fall distance of 1000m Feingold's scheme appears to be in better agreement with the observations than the parametrization derived above (w=0 curve plotted) for a rainfall rate of 0.26mm/hr although the shape of the curve of eqn (47) is different from that suggested by the observational data which agrees with the parametrization here. Improved agreement is seen for the parametrization presented in this paper when a non-zero vertical velocity is included for low rainfall rates. For large rainfall rates the scheme of Feingold is in worse agreement with the observations.

6. IMPACT OF EVAPORATION UPON A GCM

Previous sections have noted the different evaporation rates for rain and snow. Here the impact of that difference upon the simulation of climate by a general circulation model is briefly addressed.

The model used in the UK Meteorological Office Unified Model (the Hadley Centre Climate Model) described by Cullen (1993), used for both climate research and numerical weather prediction. A low resolution version is used with a horizontal resolution of 5x7.5° (latitude-longitude) and 19 hybrid (eta co-ordinates) levels in the vertical with a timestep of 60 minutes. The condensed water content of stratiform cloud is predicted using the statistical cloud scheme of Smith (1990).

Results from three experiments with different formulations for the evaporation of large-scale precipitation are compared. The first (A) employs the evaporation parametrization derived previously consistent with the phase of the precipitation while the second (B) uses the scheme for rain evaporation regardless of phase. The latter scheme effectively reduces the sublimation of snow by approximately half compared to the former. In a third experiment (C) the evaporation coefficient for both rain and snow set to a constant value of $2x10^{-5}s^{-1}$ (used in an earlier version of the Met. Office climate model - Slingo (1985)). This is equivalent to the evaporation of rain at a precipitation rate of 0.1mm/hr using the parametrization derived in section 3 above for a pressure of 1000mb. Results for northern winter (December, January, February-DJF) are considered being averaged over 4 winters for both experiments. Changes of similar magnitude are seen during northern summer.

Figure 9 compares zonal mean cooling due to evaporation of precipitation. Experiment A with the correct sublimation rates for snow shows larger cooling rates below 800mb in the storm tracks of both hemispheres. This leads to increased low level cloudiness as seen in the zonal mean height-latitude cross-section of the difference in cloud cover between experiments A and B (fig 10). Amounts in experiment A are up to 7% larger in the southern hemisphere trough (as defined by the mean sea level pressure of fig 11(b)), a fractional increase of 20% over cloud amounts seen in experiment B. This leads to an increase in the top of atmosphere albedo when snow evaporation is included, up to 10% locally (55°S, 10°W - fig 11(a)) and around 1% in the zonal mean between 40 and 70°S (figure 12) increasing the difference against ERBE data (a four year mean for DJF between 1985/86 and 1988/89). Increases of up to 3% in the zonal mean are found in the storm track regions of the northern hemisphere.

Using a fixed evaporation rate (experiment C - not shown) gives little systematic difference

to experiment B. Cooling due to evaporation in the zonal mean is similar. Increases in cloud amounts (upto 3%) are seen in the upper troposphere of the mid-latitudes. In these regions cloud ice water contents are typically 10^{-3} g/kg giving precipitation rates of around 2×10^{-3} mm/hr, less that that associated with the fixed evaporation coefficient used. No systematic signal is seen in the top of atmosphere albedo.

7. SUMMARY

Consistent parametrizations for the evaporation of rain and snow have been derived. Comparison against the detailed calculations of Clough and Frank (1991) show good agreement for the evaporation of rain when a gamma distribution of order unity rather than a Marshall-Palmer distribution is used to describe the drop size spectrum. Clough and Frank (1991) report that small drops evaporate relatively more quickly than larger ones, and so the population of drop sizes will deviate from that of Marshall and Palmer. For rain the scheme compares well with others schemes recently reported. For convective precipitation accounting for the sub-grid scale variability within the rain area makes little difference to the evaporation rates estimated but the inclusion of the effect of vertical velocity does bring the scheme into better agreement with radar observations of precipitation reduction by evaporation below cloud base. However it should be noted that the uncertainty in the observations is large.

For snow, the agreement between the parametrization and results of Clough and Frank (1991) is also reasonable, the larger sublimation rates for snow being noted. Comparison against an alternative parametrization based upon observations indicates the need for further work in the area of snow sublimation. The differences between the scheme derived here and that of

Heymsfield and Donner (1990) grow as temperature decreases. Differences do not appear to be accounted for by the assumed shape of the snow crystals but it is noted that the scheme derived here is sensitive to assumptions regarding the particle concentration, a quantity whose value and variation with temperature and mass of precipitation is poorly known from either observations or detailed microphysical modelling. Further work in this area is required; more certain parametrizations of snow sublimation will only be achieved by the inclusion of such sensitivities.

The impact of the greater rate of evaporation of snow from stratiform clouds upon present day climate has been indicated using a low resolution version of the UK Met. Office Unified Model with increased cloudiness and top of atmosphere albedo in the storm tracks of both northern and southern hemisphere during northern winter.

Inclusion of different parametrization for the evaporation of falling snow in NWP models is probably also of importance. Thorpe and Clough (1991) attribute the formation of downdraughts below regions of frontal ascent to the higher rate of snow evaporation. It is also likely to be of importance in the generation of convective scale downdraughts which form near the freezing level. The larger cooling rates associated with the evaporation of snow may generate greater negative buoyancies and so more vigorous downdraughts impacting on the structure and energy budget of the boundary layer in the tropics. Such changes may cause larger modifications to the simulated global circulation than those reported in the study above. Some of these issues will be addressed in a later paper.

8. ACKNOWLEDGMENTS

My thanks to the stimulation of Peter Rowntree who alerted me to the possibility of the analysis in section 2 and 3 many years ago, to an anonymous reviewer who pointed out deficiencies in the parametrization of snow sublimation in an earlier draft of the paper.

9. REFERENCES

Bower, K.N., Moss, S.J., Johnson, D.W., Choularton, T.W., Latham, J., Brown, P.R.A., Blyth, A.m. and Cardwell, J., 1995 : A Parametrization of the Ice Content Observed in Frontal and Convective Clouds, Submitted to the Q.J.R.Meteorol.Soc.

Clough, S.A. and Franks,R.A.A., 1991 : The evaporation of frontal and other stratiform precipitation., Q.J.R.Meteorol.Soc., **117**, 1057-1080

Cox, G.P., 1988 : Modelling precipitation in frontal rainbands., Q.J.R.Meteorol.Soc., **114**, 115-127

Cullen, M.J.P., 1993 : The Unified Forecast/Climate Model., Meteorological Magazine, **112**, 81-94

Curić, M. and Janc, D., 1988 : A Forced 1-D Convective Cloud Model, Meteorol. Atmos. Phys., **39**, 51-62

Dolman, A.J. and Gregory, D., 1992 : The parametrization of rainfall interception in GCMs., Q.J.R.Meteorol.Soc., **118**, 455-467

Feingold, G., 1993 : Parametrization of evaporation of rainfall for use in general circulation models., J.Atmos.Sci., **50**, 3454-3467

Frösling, N., 1938 : Über die verdunstung fallender Tropfen., Gerlands Beitr. Geophys., **52**, 170

Gregory, D. and Rowntree, P.R. 1990 : A mass flux convection scheme with representation of cloud ensemble characteristics and stability dependent closure., Mon. Wea. Rev., **118**, 1483-1506

Gunn, K.L.S. and Kinzer, G.D. 1949 : The terminal velocity of fall for water droplets in stagnant air., J.Meteorol., **6**, 243-251

Heymsfield, A.J., 1977 : Precipitation development in stratiform ice clouds: a microphysical and dynamical study., J.Atmos.Sci., **34**, 367-382

Heymsfield, A.J. and Donner, L.J., 1990 : A scheme for parametrizing ice-water content in general circulation models., J.Atmos.Sci., **47**, 1865-1877

Houze, R.A.,Jr., Hobbs, P.V., Herzegh, P.H. and Parsons, D.B., 1979 : Size distribution of precipitation particles in frontal clouds., J.Atmos.Sci., **36**, 156-162

Kessler,E., 1969 : On the distribution and continuity of water substance in atmospheric circulations., Met. Monographs, **10**, N°.32, A.Met.Soc., 82pp

Locatelli, J.D. and Hobbs, P.V., 1974 : Fall speeds and masses of solid precipitation particles., J.Geophys.Res., **79**, 2185-2197

List, R. E., 1951 : Smithsonian Meteorological Tables, (sixth Edition)., 527pp, The Smithsonian Institution

Liu, Y.J. and Orville, H.D., 1969 : Numerical modelling of precipitation and cloud shadow effects on mountain induced cumuli., J.Atmos.Sci., **26**, 1283-1298

Marshall,J.S. and Palmer, W.Mc.K., 1948 : The distribution of raindrops with size., J.Meteor., **5**, 165-166

Pruppacher, H.R. and Klett, J.D., 1978 : Microphysics of Clouds and Precipitation., D. Reidal Publishing Company

Rogers, R.R and Yau, M.K., 1989 : A short course in cloud physics., Pergamon Press, 3rd Ed., 293pp

Rosenfeld, D. and Mintz, Y.M., 1988 : Evaporation of rain falling from convective clouds as derived from radar measurements., J.App.Meteorol., **29**, 209-215

Ryan, B., 1995 : The Nature of Precipitating Layer Clouds Around the World., Joint GCSS/ECMWF workshop on Layer Clouds : Modellling, Observations and Data Assimulation., 31 Sept - 3 Oct 1994, ECMWF, Shinfield Park, Reading, UK.

Schlesinger, M.E., Oh, J.-E. and Rosenfeld, D., 1988 : A parametrization of evaporation of rainfall., Mon.Wea.Rev., **116**, 1887-1895

Senior, C.A. and Mitchell, J.F.B., 1993 : Carbon Dioxide and Climate : The Impact of Cloud Parametrization., J. of Climate, **6**, 393-417

Slingo, A. (Ed), 1985 : Handbook of the Meteorological Office 11-layer atmospheric general circulation model. Volumn 1 : Model Description., Dynamical Climatology Technical Note No. 29, Available from the Hadley Centre for Climate Prediction and Research, Meteorological Office, London Road, Bracknell, Berks. RG12 2SZ

Smith, R.N.B., 1990 : A scheme for predicting layer clouds and their water content in a general circulation model., Q.J.R.Meteorol.Soc., **116**, 435-460

Srivastava, R.C., 1985 : A simple model of evaporatively driven downdraft: Application to microburst downdraft., J.Atmos.Sci., **42**, 1004-1023

Sundqvist, H., 1988 : Parametrization of condensation and associated clouds in models for weather prediction and general circulation simulation., Physically based modelling and simulation of climate and climate change, Vol I, M.E.Schlesinger, Ed., Reidel, 433-462

Thorpe, A.J. and Clough S.A., 1991 : Mesoscale dynamics of cold fronts: Structures described by dropsoundings in FRONTS87., Q.J.R.Meteorol.Soc., **117**, 903-941

Thorpe, A.D. and Mason, B.J., 1966 : The evaporation of ice spheres and ice crystals., J.App.Phys., **17**, 541-548

Warrilow, D.A., Sangster, A.B. and Slingo, A., 1986 : Modelling of land surface processes and their influence on european climate., Dynamical Climatology Technical Note N°38, available from Hadley Centre, Meteorological Office, London Road, Bracknell, Berks. RG12 2SY UK.

UK Meteorological Office, 1964 : Hydrometric Tables. Part III. Aspirated Psychrometer Readings, Degrees Celsius (Second Edition)., 90pp, Her Majestys Stationary Office.

U.S. Government Printing Office, 1976 : U.S. Standard Atmosphere, 1976., NOAA-S/T76-1562., U.S. Government Printing Office, Washington, D.C..

Ulbrich, C. W., 1983 : Natural variations in the analytical form of the raindrop size distribution., J. Clim. and Appl. Meteor., **22**, 1764-1775

9. APPENDIX 1. Derivation of approximate formula for evaporation

A1.1 Water

Kinzer and Gunn (1951) provide estimates of

$$D_a(T,p)(\rho_V-\rho_{VS}(T_w)) \qquad \text{(A1)}$$

(as a function of temperature (T) and relative humidity (U) at a pressure of 1000mb) for water droplets assuming the temperature of the drop is equal to the ventilated wet bulb temperature (Table A1).

Calculation of T_w requires iteration and so it would be more computationally efficient to express the vapour density deficit in terms of temperature, that is to write equation (A1) in the form;

$$A_V(T,p)(\rho_V-\rho_{VS}(T)) \qquad \text{(A2)}$$

Dividing the values of equation (A1) by values of $(\rho_v-\rho_{vs}(T))$ estimated from Hydrometric Tables, Part III (1964) gives $A_V(T)$ defined by equation (A2) (table A2). The right hand column of table A2 is the mean value of A_V over all humidities. These values are used to fit the quadratic of equation (4a). Errors of less than 5% are introduced by the neglect of the humidity variation. The pressure dependency is introduced as the value of the diffusivity of water is inversely proportional to pressure. As noted above, Kinzer and Gunn's calculations were valid for a pressure of 1000mb , which is used as the reference pressure in the adjustment.

A1.2 Ice

Using values of the diffusivity of water vapour over ice (List, 1951) and values of ventilated ice bulb temperature (T_i) estimated from Hydrometric Tables, Part III (1964), $D_a(T,p)(\rho_v-\rho_{vs}(T_i))$ can be calculated (table A3). Again values of the diffusivity of water at a pressure of 1000mb are used. Dividing these values by $(\rho_v-\rho_{vs}(T))$ gives $A_v(T)$ (defined by equation (A2) relevant to ice. The right hand column of table A4 is the mean value of A_v for ice over all humidities. These values are used to fit the quadratic of equation (4b). As for water, errors of less than 5% are introduced by the neglect of the humidity variation. A pressure variation has been included as discussed in the previous section above.

Figure 1 Rate of change of precipitation mass with time for the Gregory parametrisation of the evaporation of (a)rain ((- - -) using a Marshall-Palmer drop size distribution, (— —) using a gamma distribution of order unity to represent the drop size distribution and (b)snow (- - -) compared against the detailed calculations of Clough and Frank (1991) (——).

Figure 2 Rate of change of rain mass with distance due to the Gregory (——), Sundqvist (— —) and Schlesinger (- - -) schemes.

Figure 3 Fall depth for evaporation for 50% of initial snow mass as a function of temperature, relative humidity 300m below cloud base and initial snow mass for the Gregory scheme and that of Heymsfield and Donner. (----):20%, (.....):40%, (- - -):60% and (— —):80% relative humidity.

Figure 4 As figure 3 but with dependency of particle concentration as a function of temperature included into the Gregory scheme.

Figure 5 Fall depth for evaporation of 50% of initial rain mass at 0°C as a function of relative humidity and initial rain mass for the Gregory scheme and that of Heymsfield and Donner. Key to curves : as figure 3

Figure 6 Fraction of rain remaining as a function of distance below cloud base for six rainfall rates at cloud base (Pb) from the observations of Rosenfeld. x show observed data and —.— the error limits of the observations, - - - using basic Gregory scheme and — — — for the

Gregory scheme incorporating sub-grid variability of rainfall.

Figure 7 As figure 6 but impact of downward vertical velocity on evaporation of rain as predicted by the Gregory scheme with the sub-grid scale variability of rainfall accounted for. w=0 (——), 5 (— — —) and 10m/s (- - -)

Figure 8 As figure 6 but comparing the Gregory scheme (——, w=0) with that of Feingold (— — —).

Figure 9 Cooling due to the evaporation of large-scale precipitation for DJF with both rain and snow evaporation included (experiment A) and all evaporation treated as for rain (experiment B).

Figure 10 Height latitude diagrams for DJF showing (a) stratiform cloud amount for experiment A and (b) differences in stratiform cloud amount (%) between experiments A and B.

Figure 11 (a) Change in top of atmosphere albedo between experiments A and B and (b) mean sea level pressure for experiment A for DJF.

Figure 12 Zonal mean top of atmosphere albedo for DJF with experiment A (—·—) and B (- - -) compared to albedo from ERBE (——) (4 year mean of DJF for 1985/86 to 1988/89).

List of Tables

Table 1 Comparison of the time (secs) for the evaporation of 95% of the initial mass of precipitation for calculations of Clough and Franks (1991) and parametrisation of evaporation.

Table A1 $D_*(T)(\rho_v-\rho_{vs}(T_w))$ as calculated by Kinzer and Gunn (1951).

Table A2 Values of the coefficient A_v for water as a function of temperature and relative humidity.

Table A3 Values of $D_*(T)(\rho_v-\rho_{vs}(T_i))$.

Table A4 Values of the coefficient A_v for ice as a function of temperature and relative humidity.

Table 1 Comparison of the time (secs) for the evaporation of 90% of the initial mass of precipitation for calculations of Clough and Franks (1991) and parametrization of evaporation.

Initial precipitation rate = 1mm/hr

	Rain	Snow
Clough and Franks (1991)	760	330
Parametrization (MP)	580	240
Parametrization (Γ)	760	

MP : drop size distribution described by Marshall-Palmer distribution.
Γ : drop size distribution described by a gamma function of order unity.

Table A1 $D_s(T)(\rho_v-\rho_{vs}(T_w))$ (10^{-4} $gm^{-1}s^{-1}$) as calculated by Kinzer and Gunn (1951).

T (°C)	U(%)					
	40	50	60	70	80	90
0	0.41	0.34	0.27	0.20	0.14	0.07
10	0.65	0.54	0.43	0.32	0.21	0.11
20	0.95	0.78	0.63	0.46	0.31	0.16
30	1.32	1.09	0.86	0.64	0.42	0.21
40	1.75	1.45	1.15	0.85	0.56	0.28

Table A2 Values of the coefficient A_V (10^{-5} m^2s^{-1}) for water as a function of temperature and relative humidity.

T (°C)	U(%)						$A_v^w(I)$
	40	50	60	70	80	90	
0	1.409	1.405	1.392	1.379	1.392	1.367	1.391
10	1.153	1.149	1.144	1.135	1.111	1.160	1.142
20	0.915	0.902	0.910	0.886	0.896	0.919	0.905
30	0.724	0.718	0.708	0.703	0.691	0.691	0.706
40	0.570	0.566	0.562	0.553	0.547	0.547	0.558

Table A3 Values of $D_a(T)(\rho_v-\rho_{vs}(T_i))$ (10^{-4} $gm^{-1}s^{-1}$).

T (°C)	U(%)					
	40	**50**	**60**	**70**	**80**	**90**
-30	0.027	0.019	0.012			
-20	0.077	0.059	0.041	0.023		
-10	0.188	0.152	0.112	0.077	0.038	
0	0.384	0.322	0.255	0.191	0.120	0.059

Table A4 Values of the coefficient A_v (10^{-5} m^2s^{-1}) for ice as a function of temperature and relative humidity.

T (°C)	U(%)						$A_v^S(T)$
	40	50	60	70	80	90	
-30	1.719	1.700	1.805				1.741
-20	1.696	1.752	1.779	1.701			1.732
-10	1.572	1.580	1.560	1.577	1.504		1.559
0	1.320	1.329	1.315	1.314	1.238	1.217	1.289

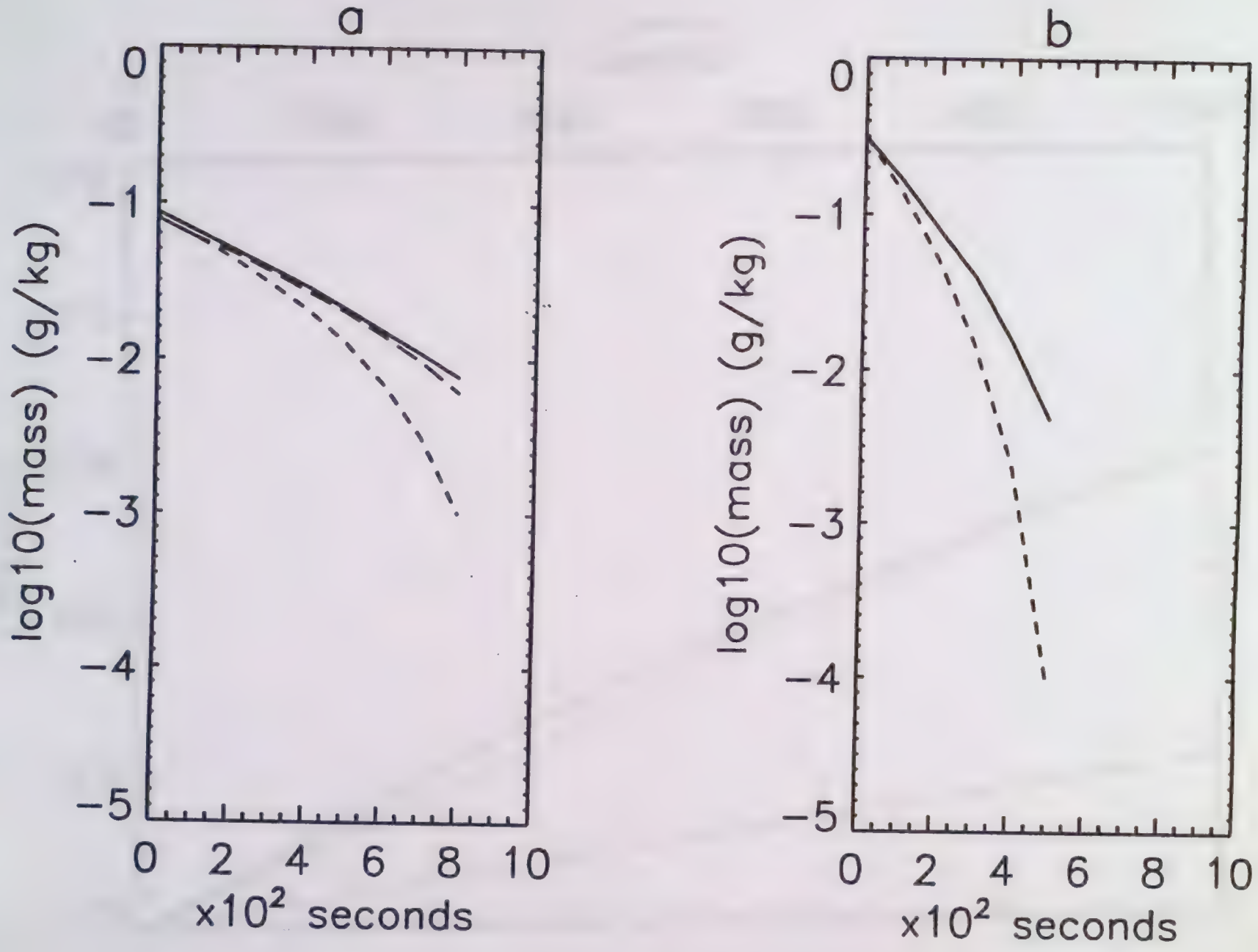

Figure 1

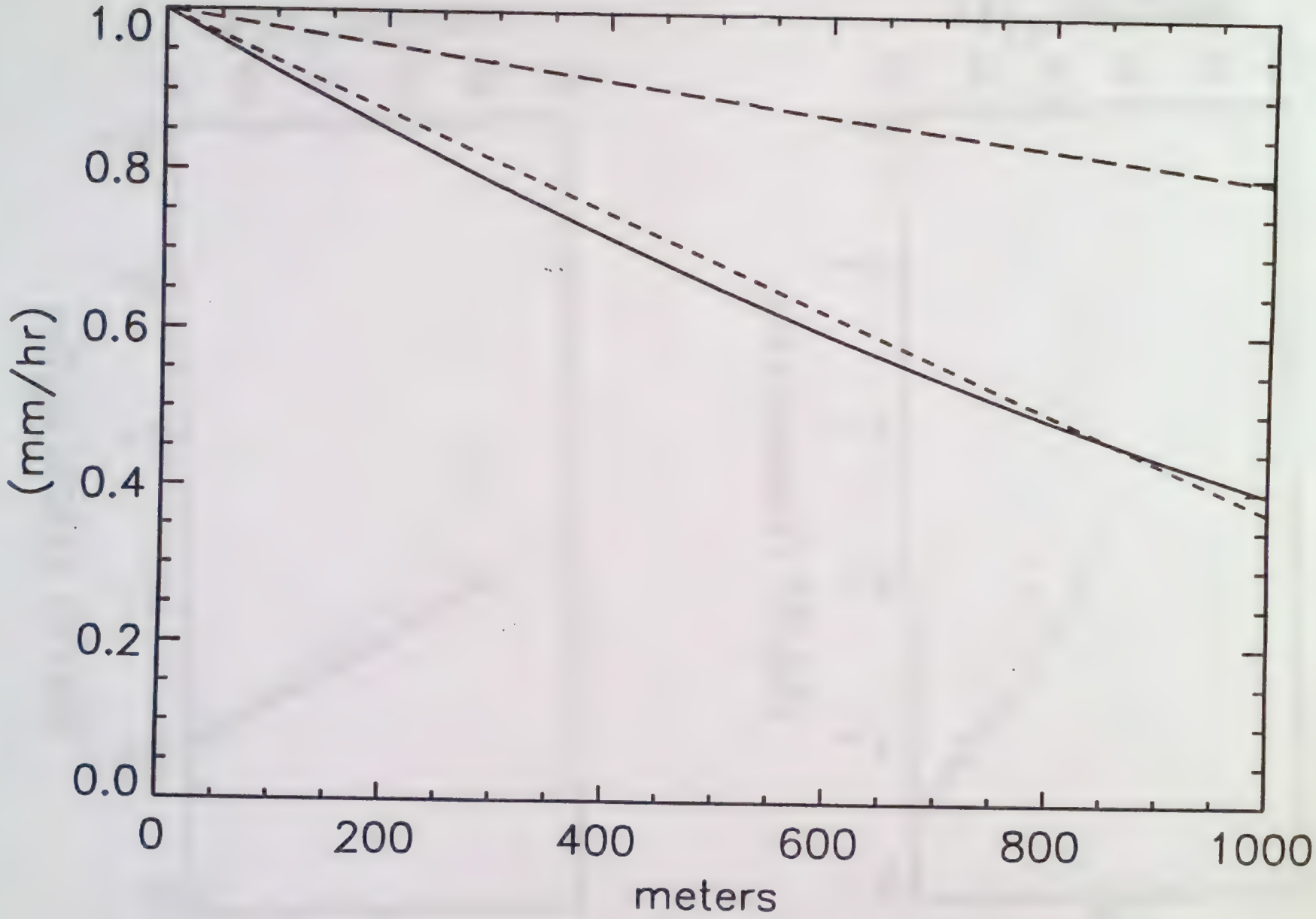

Figure 2

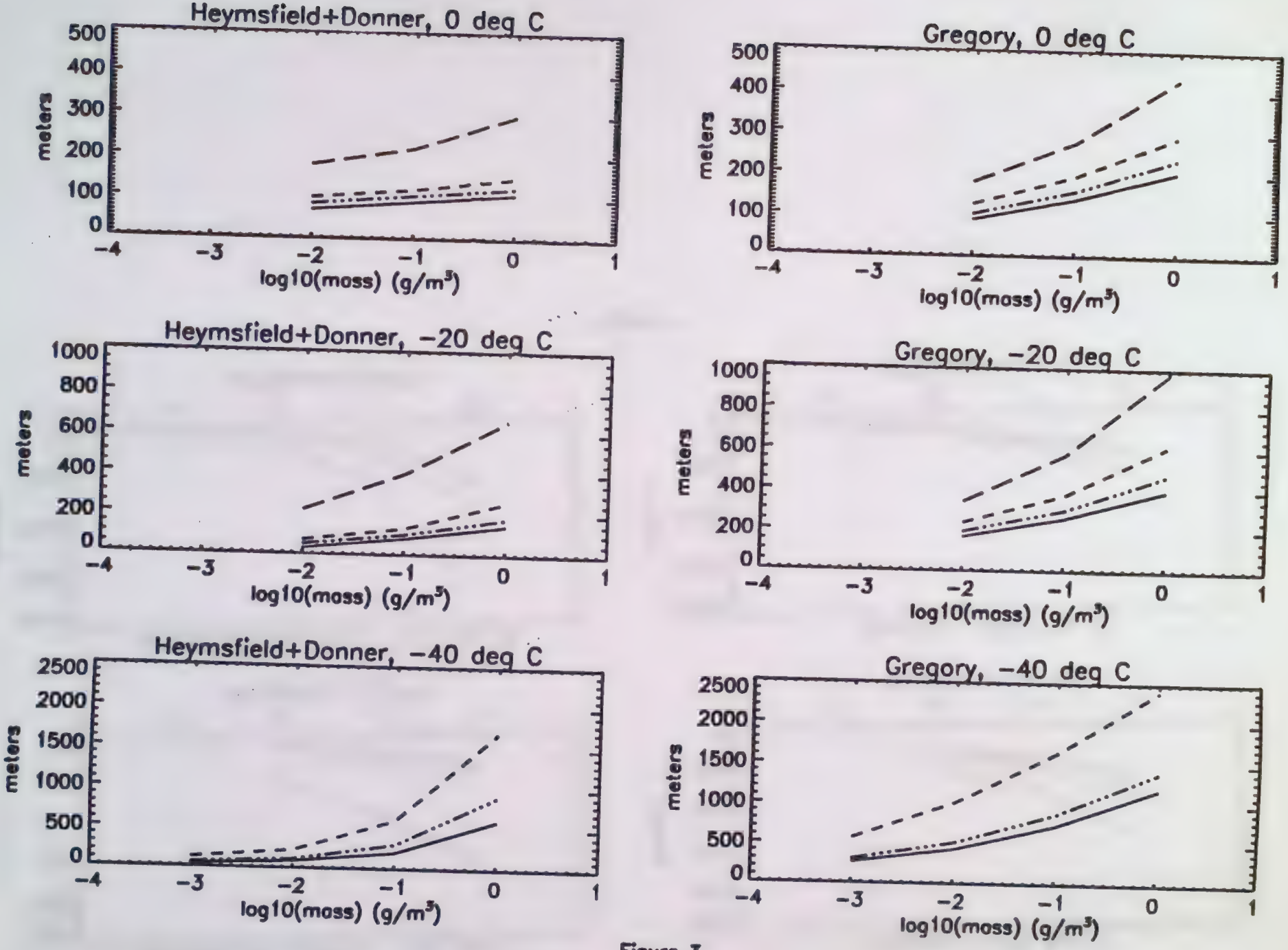
Heymsfield+Donner, 0 deg C
Gregory, 0 deg C
Heymsfield+Donner, −20 deg C
Gregory, −20 deg C
Heymsfield+Donner, −40 deg C
Gregory, −40 deg C
meters
log10(mass) (g/m³)

Figure 3

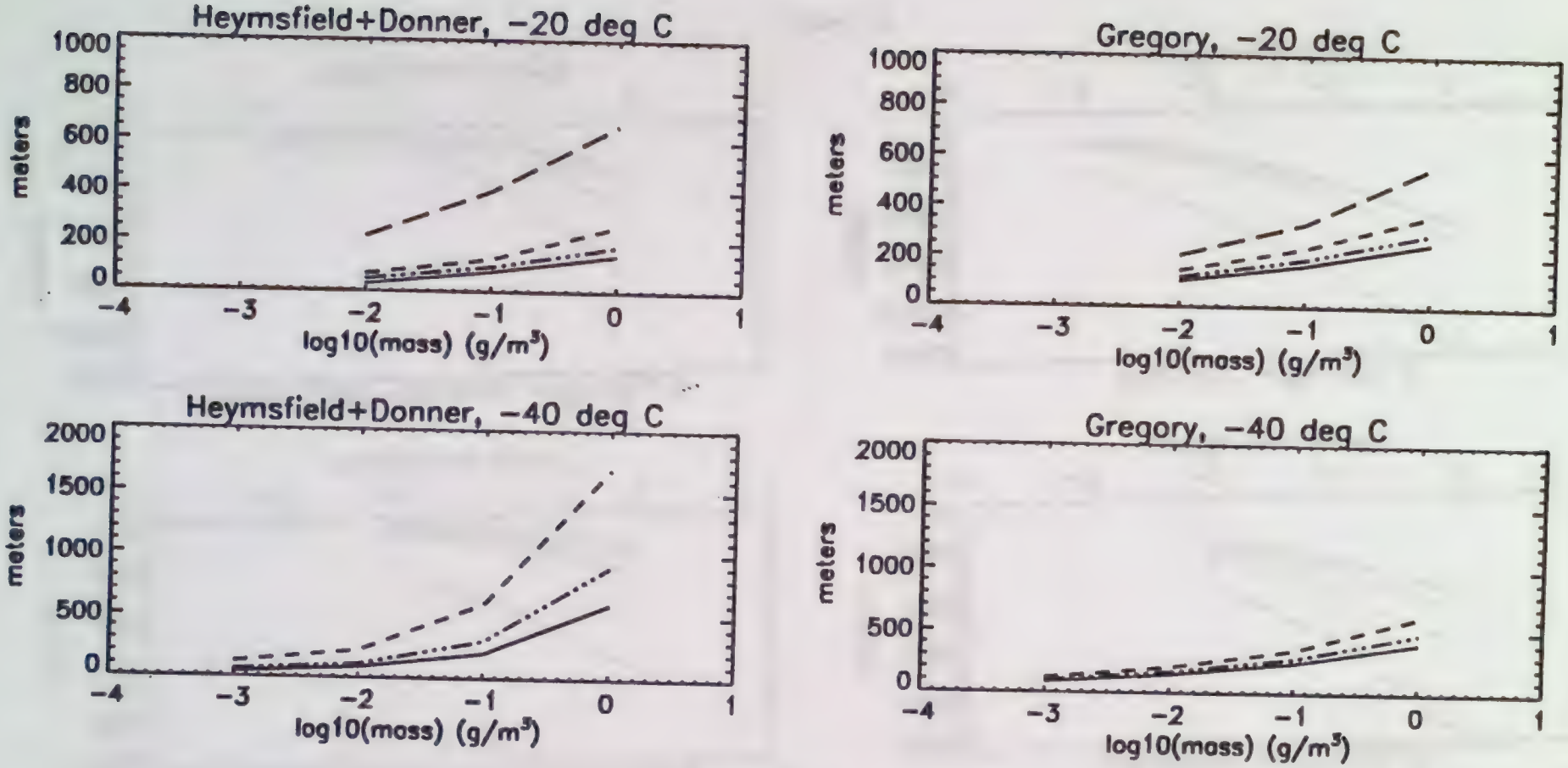
Heymsfield+Donner, −20 deg C
meters
1000
800
600
400
200
0
−4
−3
−2
−1
0
1
log10(mass) (g/m³)
Gregory, −20 deg C
meters
1000
800
600
400
200
0
−4
−3
−2
−1
0
1
log10(mass) (g/m³)
Heymsfield+Donner, −40 deg C
meters
2000
1500
1000
500
0
−4
−3
−2
−1
0
1
log10(mass) (g/m³)
Gregory, −40 deg C
meters
2000
1500
1000
500
0
−4
−3
−2
−1
0
1
log10(mass) (g/m³)

Figure 4

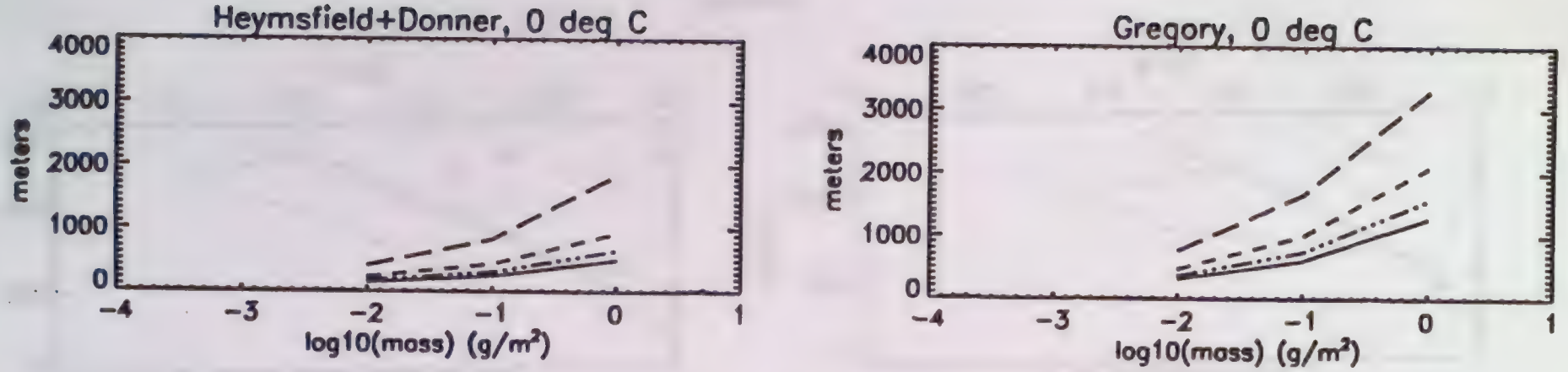
Heymsfield+Donner, 0 deg C
meters
4000
3000
2000
1000
0
-4
-3
-2
-1
0
1
log10(mass) (g/m²)
Gregory, 0 deg C
meters
4000
3000
2000
1000
0
-4
-3
-2
-1
0
1
log10(mass) (g/m²)

Figure 5

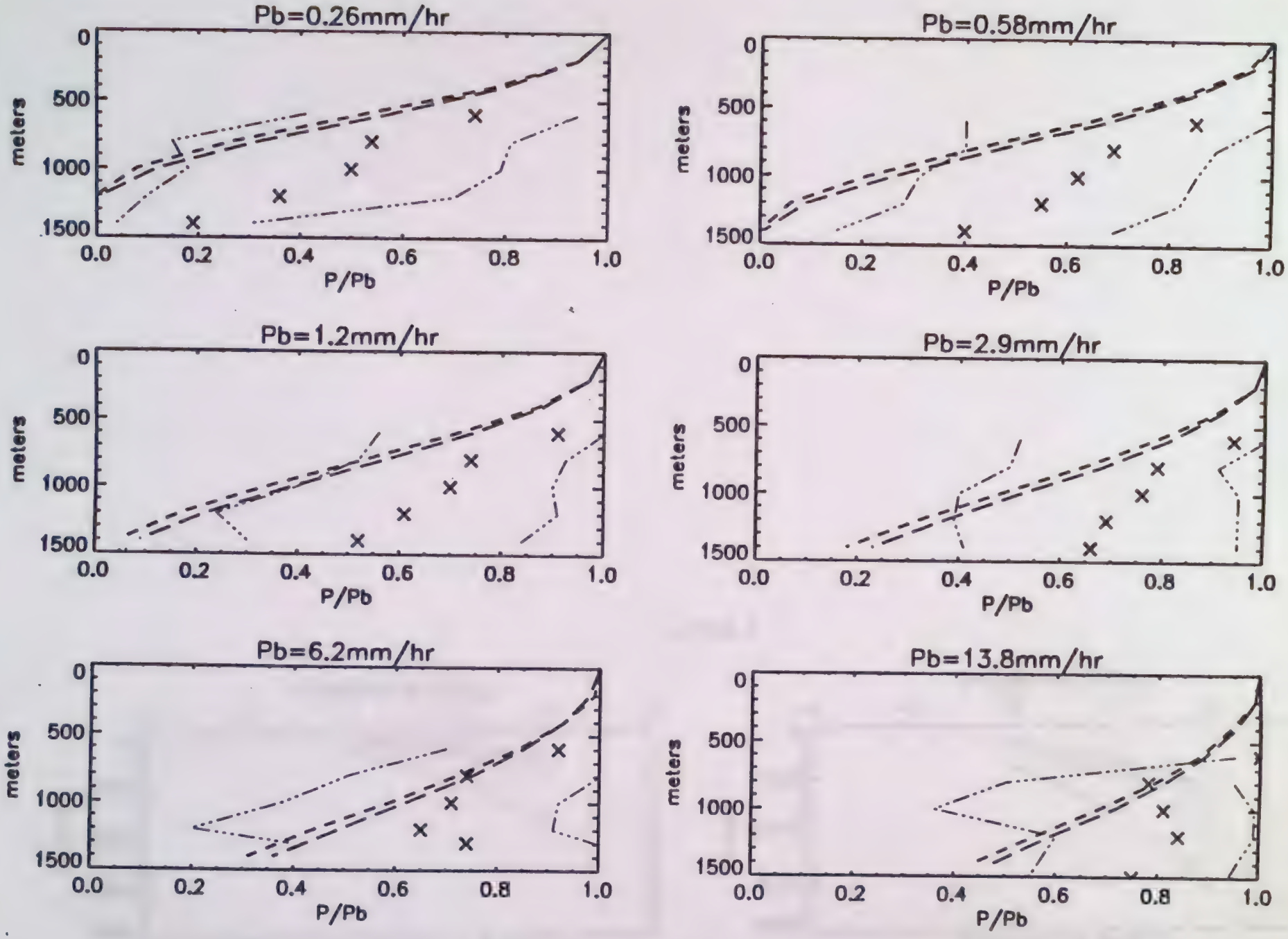
Pb=0.26mm/hr
Pb=0.58mm/hr
Pb=1.2mm/hr
Pb=2.9mm/hr
Pb=6.2mm/hr
Pb=13.8mm/hr
meters
P/Pb
0
500
1000
1500
0.0
0.2
0.4
0.6
0.8
1.0

Figure 6

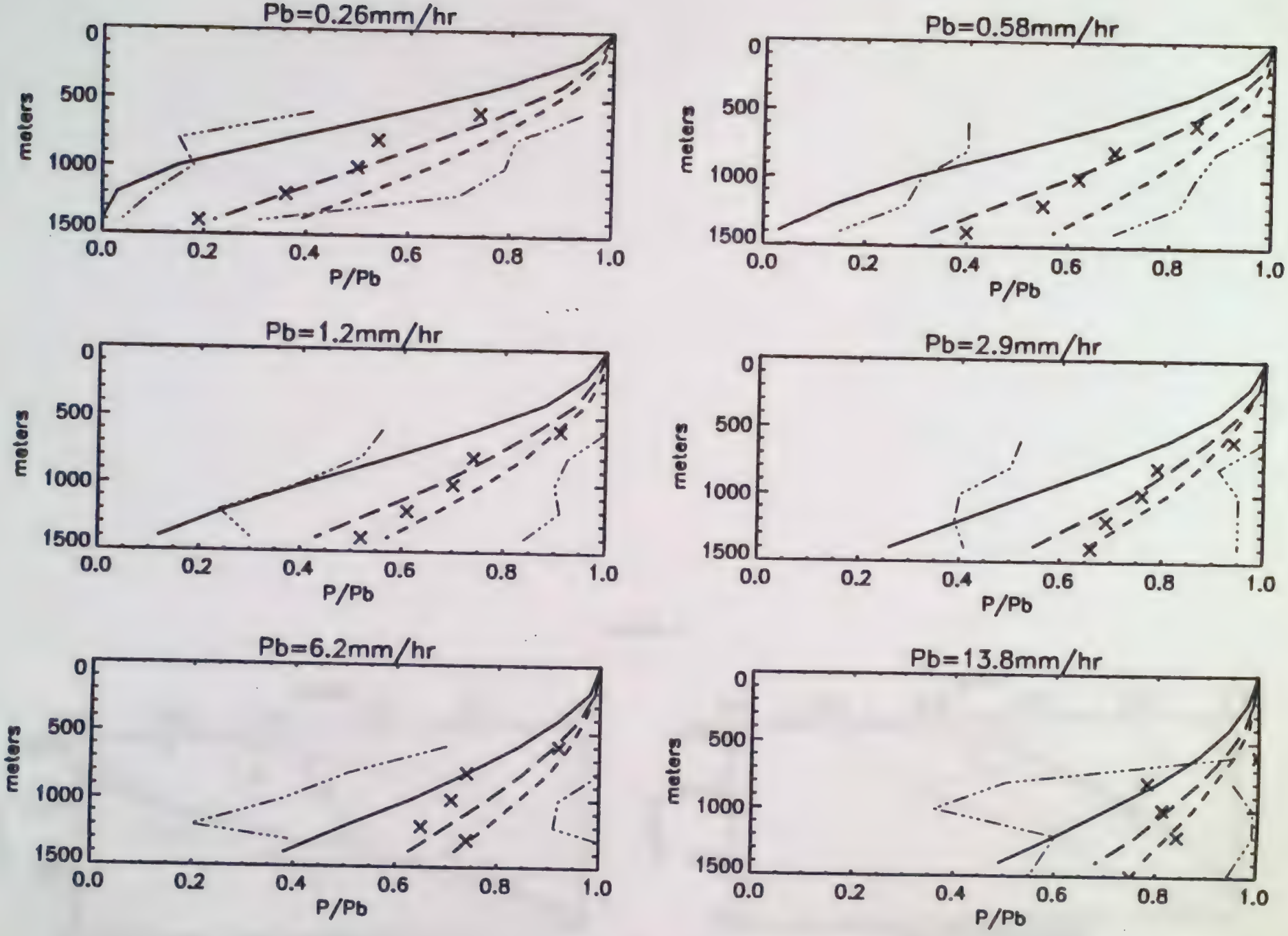
Pb=0.26mm/hr
Pb=0.58mm/hr
Pb=1.2mm/hr
Pb=2.9mm/hr
Pb=6.2mm/hr
Pb=13.8mm/hr
meters
0
500
1000
1500
0.0
0.2
0.4
0.6
0.8
1.0
P/Pb

Figure 7

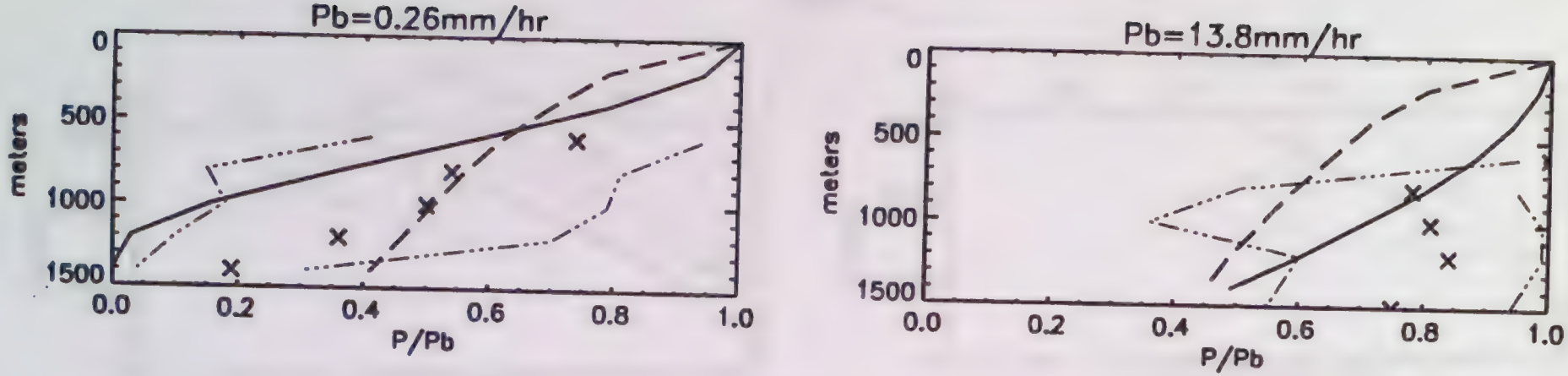
Pb=0.26mm/hr
meters
0
500
1000
1500
0.0
0.2
0.4
0.6
0.8
1.0
P/Pb
Pb=13.8mm/hr
meters
0
500
1000
1500
0.0
0.2
0.4
0.6
0.8
1.0
P/Pb

Figure 8

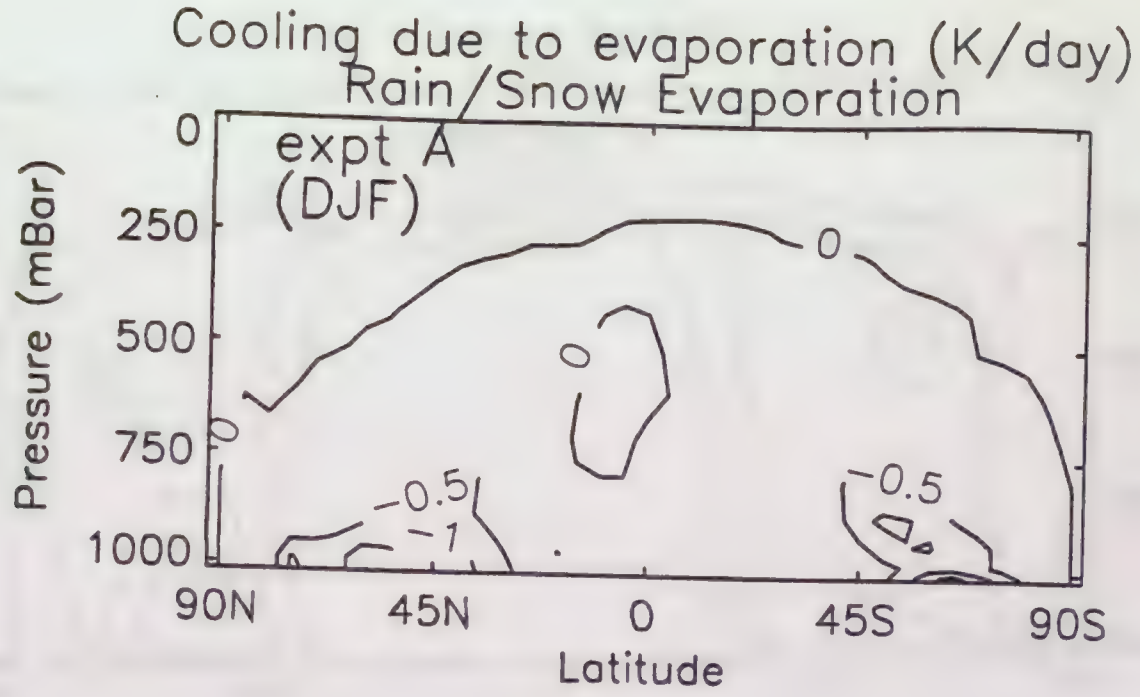
Cooling due to evaporation (K/day)
Rain/Snow Evaporation
expt A
(DJF)
Pressure (mBar)
0
250
500
750
1000
0
0
0
-0.5
-1
-0.5
90N
45N
0
45S
90S
Latitude

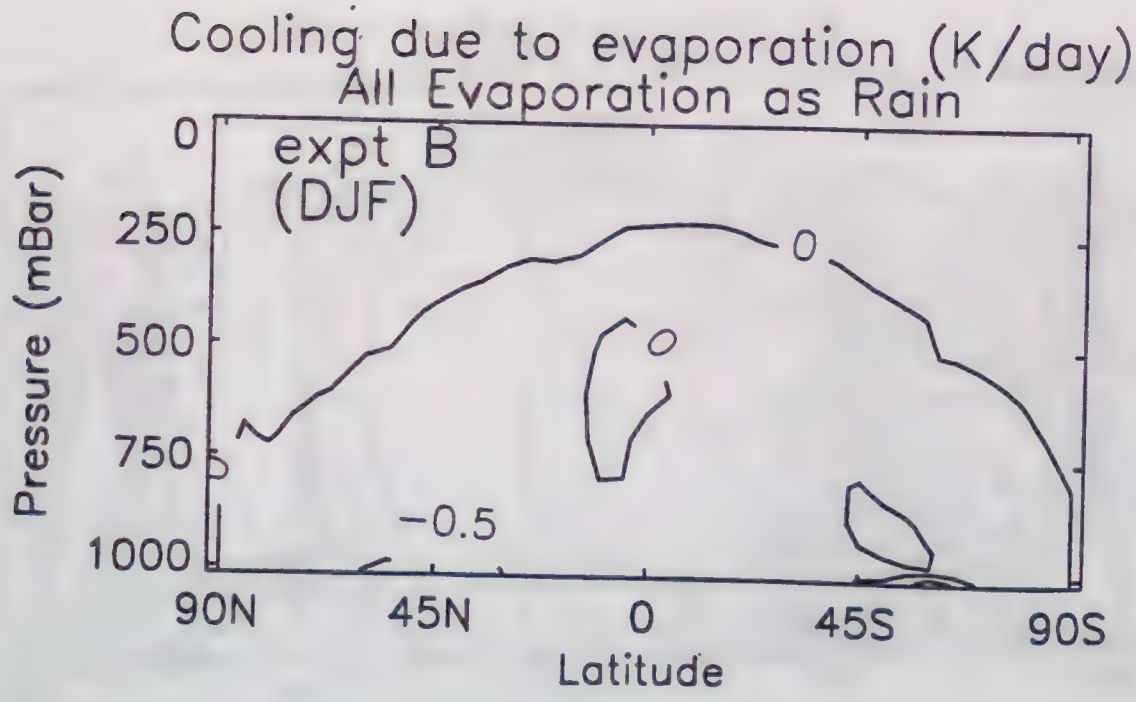
Cooling due to evaporation (K/day)
All Evaporation as Rain
expt B
(DJF)
Pressure (mBar)
0
250
500
750
1000
0
0
-0.5
90N
45N
0
45S
90S
Latitude

Figure 9

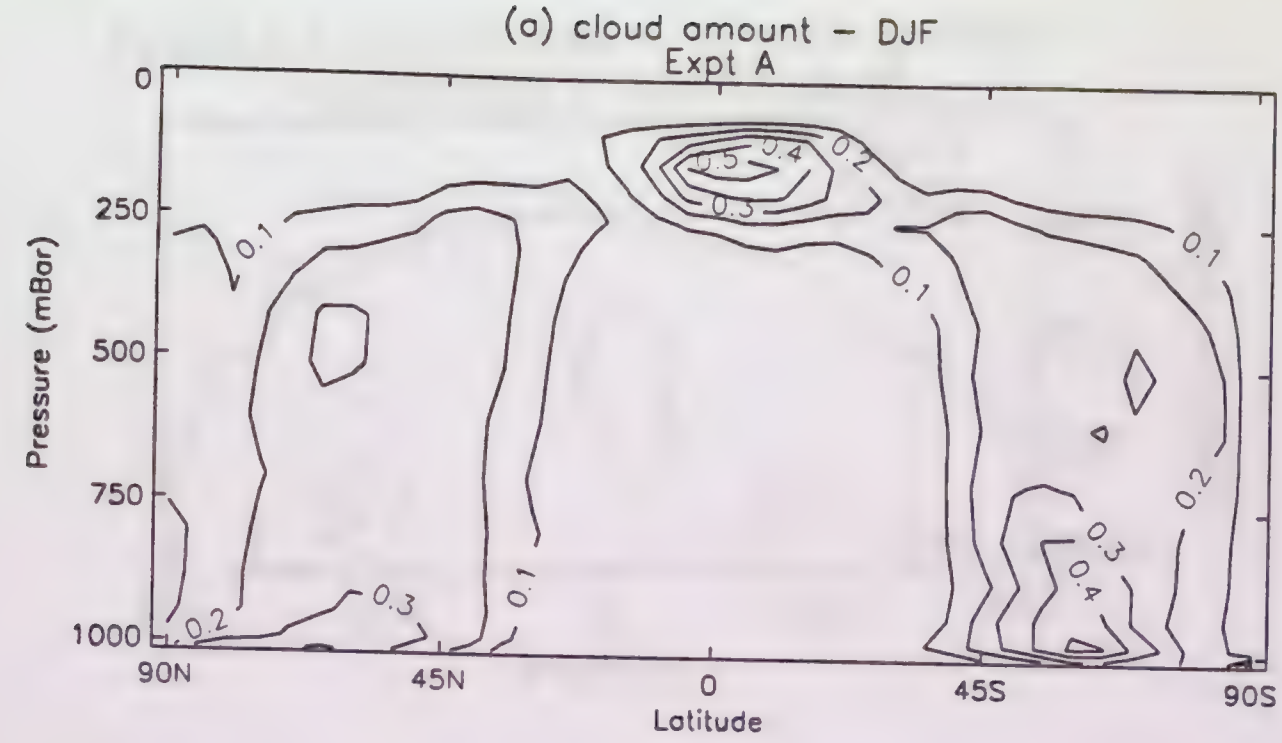
(a) cloud amount – DJF
Expt A
Pressure (mBar)
0
250
500
750
1000
90N
45N
0
45S
90S
Latitude

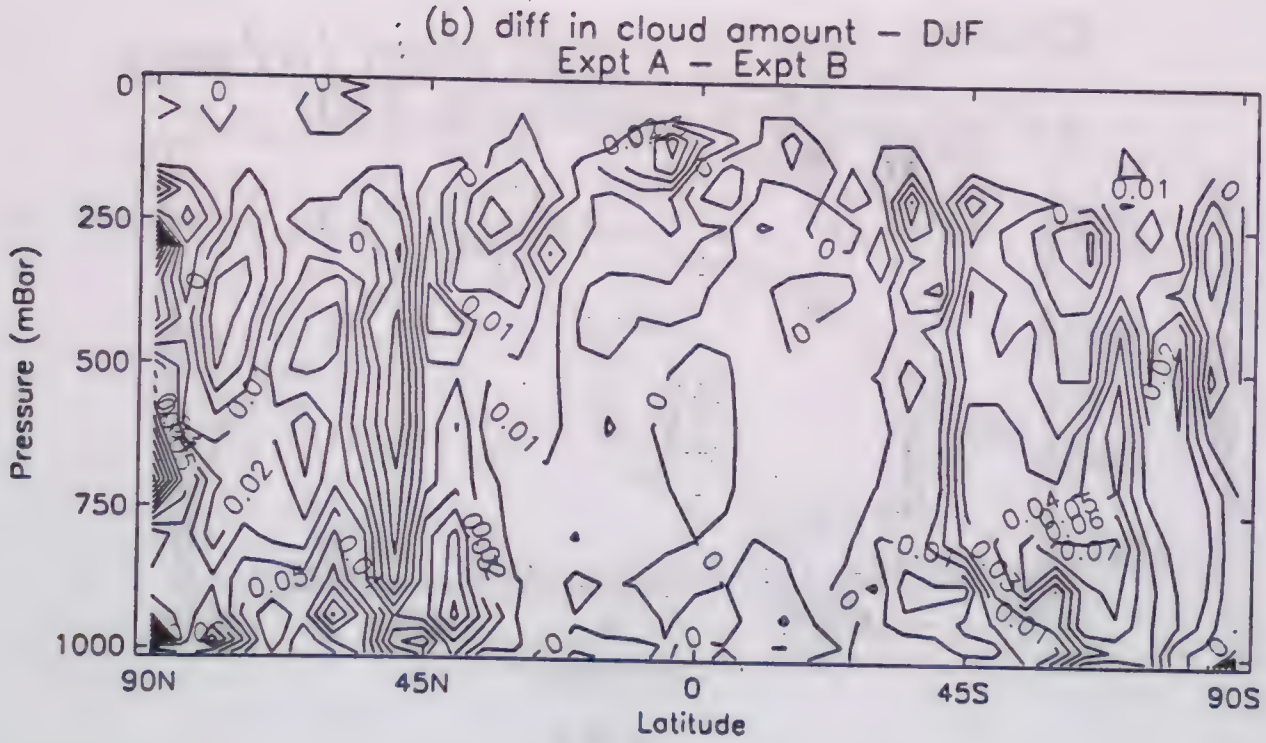
(b) diff in cloud amount – DJF
Expt A – Expt B
Pressure (mBar)
0
250
500
750
1000
90N
45N
0
45S
90S
Latitude

Figure 10

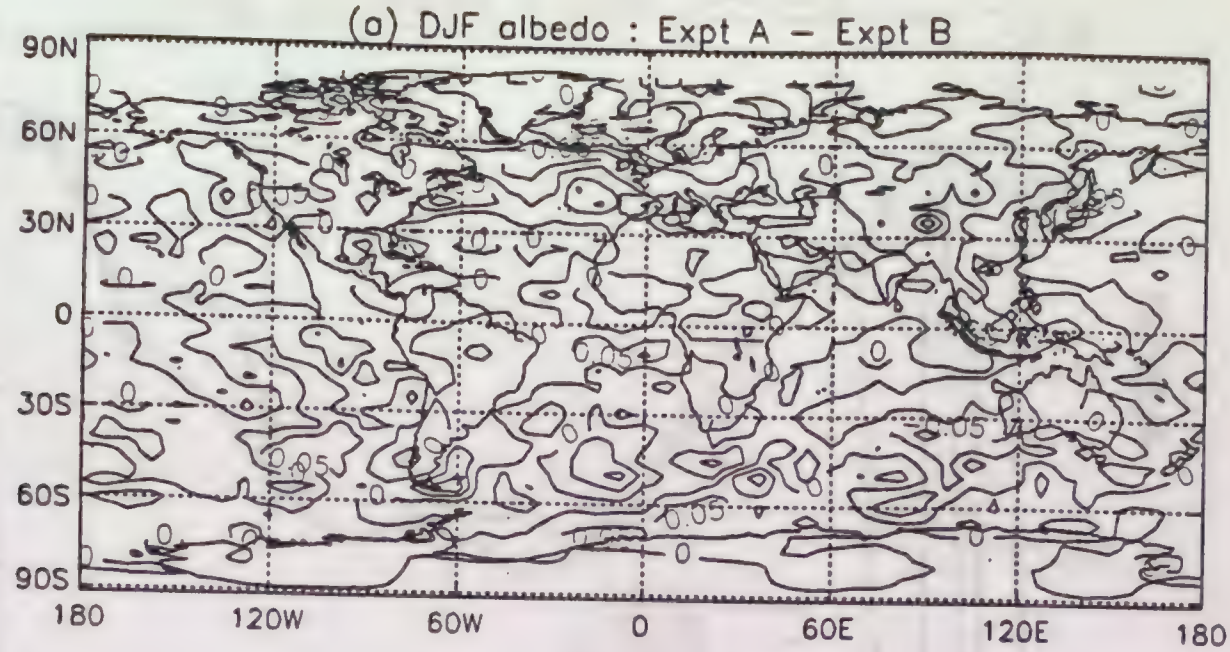
(a) DJF albedo : Expt A – Expt B
90N
60N
30N
0
30S
60S
90S
180
120W
60W
0
60E
120E
180

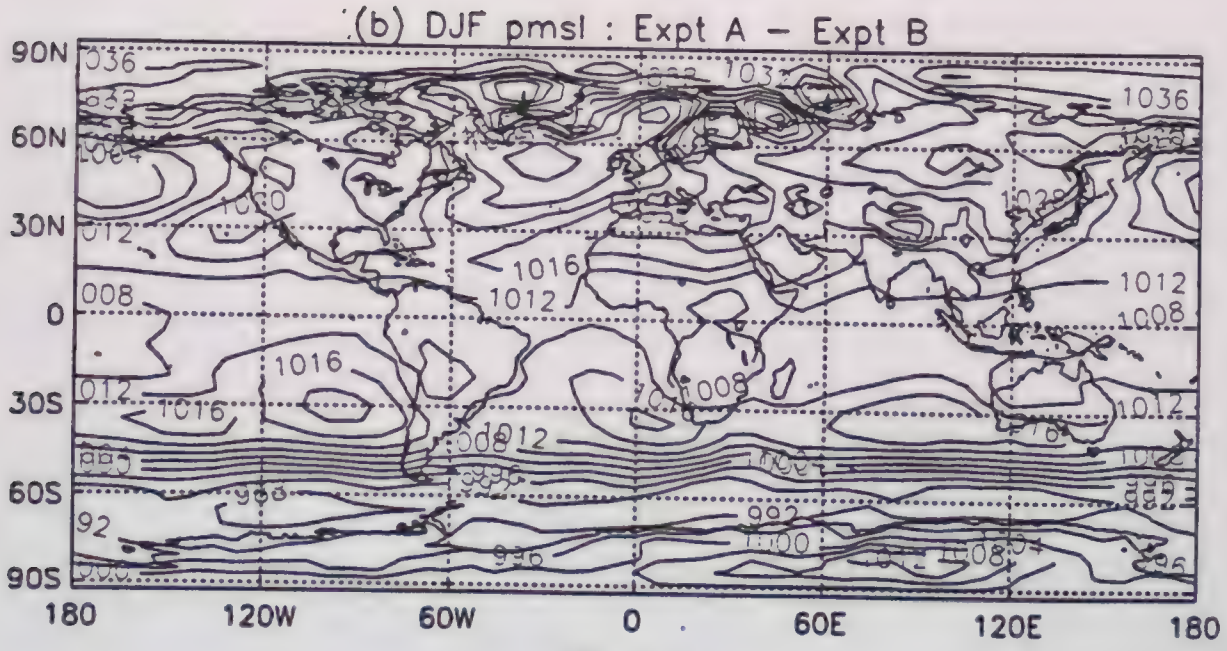
(b) DJF pmsl : Expt A – Expt B
90N
60N
30N
0
30S
60S
90S
180
120W
60W
0
60E
120E
180
1036
1012
1008
1016
992

Figure 11

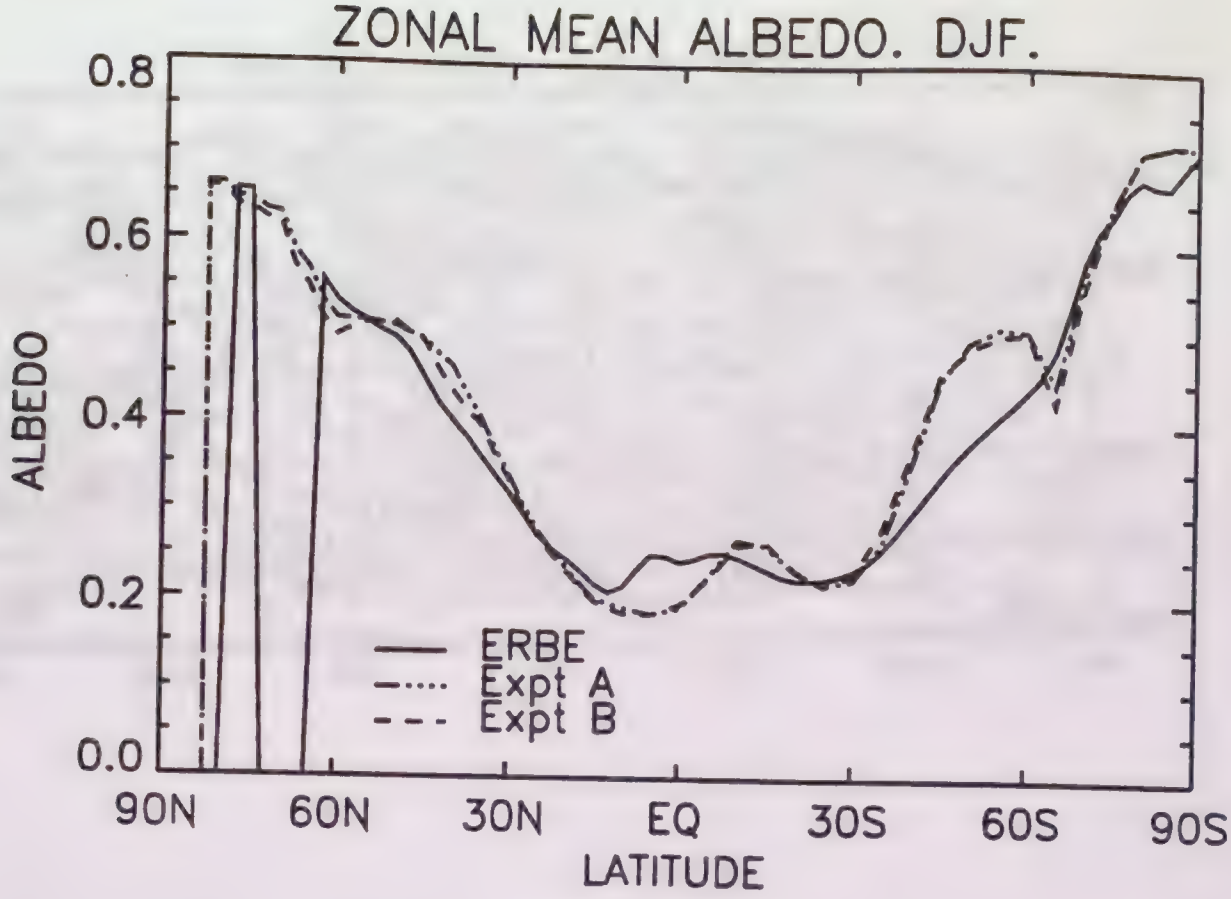
ZONAL MEAN ALBEDO. DJF.
0.8
0.6
0.4
0.2
0.0
ALBEDO
ERBE
Expt A
Expt B
90N
60N
30N
EQ
30S
60S
90S
LATITUDE

Figure 12

CLIMATE RESEARCH TECHNICAL NOTES

CRTN 1	Oct 1990	Estimates of the sensitivity of climate to vegetation changes using the Penman-Monteith equation. P R Rowntree
CRTN 2	Oct 1990	An ocean general circulation model of the Indian Ocean for hindcasting studies. D J Carrington
CRTN 3	Oct 1990	Simulation of the tropical diurnal cycle in a climate model. D P Rowell
CRTN 4	Oct 1990	Low frequency variability of the oceans. C K Folland, A Colman, D E Parker and A Bevan
CRTN 5	Dec 1990	A comparison of 11-level General Circulation Model Simulations with observations in the East Sahel. K Maskell
CRTN 6	Dec 1990	Climate Change Prediction. J F B Mitchell and Qing-cun Zeng
CRTN 7	Jan 1991	Deforestation of Amazonia - modelling the effects of albedo change. M F Mylne and P R Rowntree
CRTN 8	Jan 1991	The role of observations in climate prediction and research. D J Carson
CRTN 9	Mar 1991	The greenhouse effect and its likely consequences for climate change. D J Carson
CRTN 10	Apr 1991	Use of wind stresses from operational N.W.P. models to force an O.G.C.M. of the Indian Ocean. D J Carrington
CRTN 11	Jun 1991	A new daily Central England Temperature series, 1772-1991. D E Parker, T P Legg and C K Folland
CRTN 12	Jul 1991	Causes and predictability of Sahel rainfall variability. D P Rowell, C K Folland, K Maskell, J A Owen, M N Ward

CLIMATE RESEARCH TECHNICAL NOTES

CRTN 13	Jul 1991	Modelling changes in climate due to enhanced CO2, the role of atmospheric dynamics, cloud and moisture. C A Senior, J F B Mitchell, H Le Treut and Z-X Li
CRTN 14	Sep 1991	Sea temperature bucket models used to correct historical SST data in the Meteorological Office. C K Folland
CRTN 15	Aug 1991	Modelling climate change, and some potential effects on agriculture in the U.K. P R Rowntree, B A Callander and J Cochrane
CRTN 16	Aug 1991	The Boreal Forests and Climate G Thomas and P R Rowntree
CRTN 17	Aug 1991	Development of a Stratosphere-Troposphere Data Assimilation System. R Swinbank.
CRTN 18	Sep 1991	A study of asynchronous coupling using a simple climate model. M K Davey.
CRTN 19	Sep 1991	The Oceanic Carbon Cycle. N K Taylor
CRTN 20	Nov 1991	Worldwide ocean-atmosphere surface fields in Sahel wet and dry years using provisionally corrected surface wind data. M N Ward
CRTN 21	Dec 1991	Coupled tropical ocean global atmosphere models at the UKMO. M K Davey, C Gordon, S Ineson and S Lawrence
CRTN 22	Dec 1991	Empirical parameterisation of tropical ocean-atmosphere coupling. M Allen, M K Davey, D L T Anderson and P D Killworth
CRTN 23	Feb 1992	The temporal evolution of Equatorial Currents in the Indian Ocean D L T Anderson, D J Carrington, R A Corry and C Gordon
CRTN 24	Feb 1992	Stratospheric analyses provided by the U.K. Meteorological Office M J Bailey, A O'Neill and V D Pope

CLIMATE RESEARCH TECHNICAL NOTES

CRTN 25	Feb 1992	Modelling interannual variability in the Indian Ocean using momentum fluxes from the UKMO and ECMWF operational weather analyses. D L T Anderson and D J Carrington
CRTN 26	Mar 1992	A GCM simulation of the impact of Amazonian deforestation on climate using an improved canopy representation J Lean and P R Rowntree
CRTN 27	Mar 1992	The parameterization of rainfall interception in GCMs A J Dolman and D Gregory
CRTN 28	Jun 1992	Development of worldwide marine data eigenvectors since 1985 A W Colman
CRTN 29	Jun 1992	A tropical ocean model with reduced physics M K Davey
CRTN 30	Jun 1992	International Temperature Workshop, Boulder, Colorado, USA, 16 January 1992 Edited by D E Parker
CRTN 31	Jul 1992	Simulation of clear-sky outgoing longwave radiation over the oceans using operational analyses A Slingo and M J Webb
CRTN 32	Sep 1992	A prediction of the transient response of climate J M Murphy
CRTN 33	Nov 1992	LEPS scores for assessing climate model simulations and long-range forecasts. C K Folland
CRTN 34	Jan 1993	Stratospheric Data Assimilation System Guide Editer: R Swinbank
CRTN 35	Mar 1993	A Stratosphere-Troposphere Data Assimilation System R Swinbank and A O'Neill
CRTN 36	Mar 1993	Validation of hydrological schemes for climate models against catchment data. P R Rowntree and J Lean

CLIMATE RESEARCH TECHNICAL NOTES

CRTN 37	Apr 1993	Modelling of palaeoclimates: Examples from the recent past J F B Mitchell
CRTN 38	May 1993	A simulation of seasonality in ENSO forecast skill M K Davey, D L T Anderson and S Lawrence
CRTN 39	Jul 1993	ENSO Prediction experiments using a simple ocean-atmosphere model D-H Wu, D L T Anderson and M K Davey
CRTN 40	Sep 1993	Diagnosis of dynamic sea-surface and sea-level changes from the Cox ocean model J M Gregory
CRTN 41	Sep 1993	Seasonal variations of the clear-sky greenhouse effect: the role of changes in atmospheric temperatures and humidities M J Webb, A Slingo and G L Stephens
CRTN 42	Nov 1993	Sea-level changes under increasing atmospheric CO_2 in a transient coupled ocean-atmosphere GCM experiment. J M Gregory
CRTN 43	Dec 1993	Global and regional patterns of climate change: recent predictions for the Arctic P R Rowntree
CRTN 44	Feb 1994	The effect of changing horizontal diffusion in the atmospheric version of the unified climate model C D Hall and R A Stratton
CRTN 45	Mar 1994	Simulation of El-Niño/Southern Oscillation like variability in a global AOGCM and its response to CO_2 increase. S F B Tett
CRTN 46	Apr 1994	Global data required for monitoring climate change. D E Parker and C K Folland
CRTN 47	May 1994	Seasonal uptake of anthropogenic CO_2 in an ocean general circulation model. N K Taylor

CLIMATE RESEARCH TECHNICAL NOTES

CRTN 48	Jun 1994	A tropic-wide oscillation of boreal summer rainfall and patterns of sea-surface temperature. M N Ward, K Maskell, C K Folland, D P Rowell and R Washington
CRTN 49	Jun 1994	Simulation of the tropical Pacific using a simplified ocean model M A Balmaseda, D L T Anderson and M K Davey
CRTN 50	Sep 1994	Simulation of global mean temperature using a box-diffusion climate model P R Rowntree
CRTN 51	Sep 1994	Seasonal dependence of ENSO prediction skill M A Balmaseda, M K Davey and D L T Anderson
CRTN 52	Nov 1994	Simulation of the Indian Monsoon and Tropical Intraseasonal Variability by a General Circulation Model P M Inness and D Gregory
CRTN 53	Mar 1995	A comparison of modelled surface fluxes with climatological estimates. C Gordon and D K Wright
CRTN 54	Mar 1995	The representation of moist convection in atmospheric models. D Gregory
CRTN 55	Mar 1995	A consistent treatment of the evaporation of rain and snow for use in large-scale models D Gregory